AD-A111 540 SCIENTIFIC RESEARCH ASSOCIATES INC GLASTONBURY CT F/G 20/4
A NAVIER-STOKES SOLUTION FOR TRANSONIC FLOW THROUGH A CASCADE.(U)
JAN 82 S J SHAMROTH, H MCDONALD, W R BRILEY N00019-79-C-0558
UNCLASSIFIED R81-920007-F NL

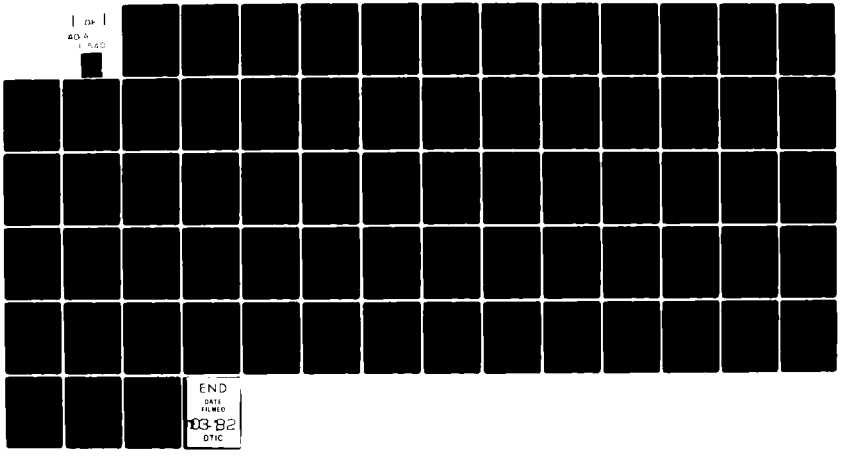

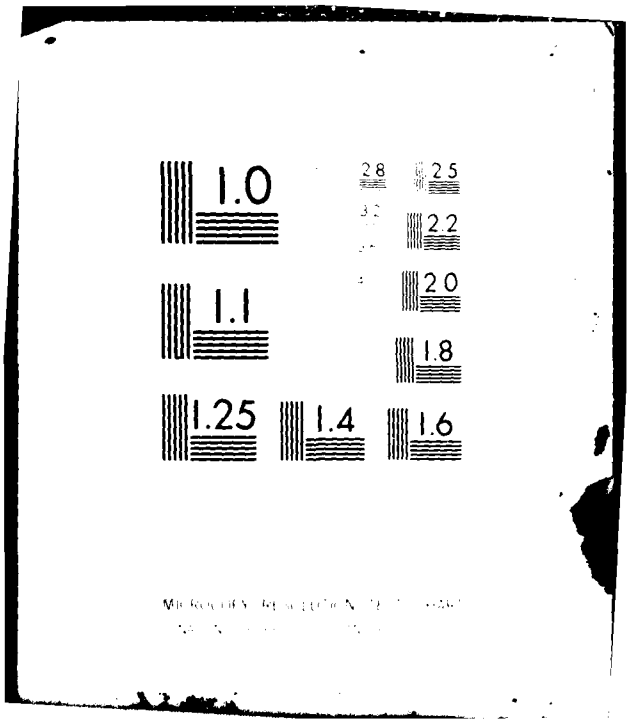
1.0
1.1
1.25
1.4
1.6
1.8
2.0
2.2
2.5

AD A111540

DTIC FILE COPY

(12)

Report R81-920007-F

A NAVIER-STOKES SOLUTION FOR TRANSONIC FLOW THROUGH A CASCADE

S. J. Shamroth, H. McDonald and W. R. Briley
Scientific Research Associates, Inc.
Glastonbury, Connecticut 06033

January 1982

Final Report
Prepared Under Contract N00019-79-C-0558

DTIC
ELECTE
MAR 3 1982
S
D
A

Prepared for
NAVAL AIR SYSTEMS COMMAND
Department of Navy

APPROVED FOR PUBLIC RELEASE
DISTRIBUTION UNLIMITED

82

Report R81-920007-F

A NAVIER-STOKES SOLUTION FOR TRANSONIC FLOW THROUGH A CASCADE

S. J. Shamroth, H. McDonald and W. R. Briley
Scientific Research Associates, Inc.
Glastonbury, Connecticut 06033

January 1982

Final Report
Prepared Under Contract N00019-79-C-0558

Prepared for
NAVAL AIR SYSTEMS COMMAND
Department of Navy

APPROVED FOR PUBLIC RELEASE:
DISTRIBUTION UNLIMITED

TABLE OF CONTENTS

DTIC COPY

1. INTRODUCTION

An understanding and quantitative knowledge of the flow through a cascade of airfoils is an important component in the gas turbine engine design process. Blade passage regions in both turbine and compressor stages are critical areas in which improper design may lead to unacceptable engine performance. Therefore a procedure capable of predicting the flow field in blade passages is an important consideration for the design engineer. One step in achieving this objective is the development of a two-dimensional cascade flow field analysis.

At the present time there are several possible approaches to the cascade flow analysis problem. These include (i) inviscid analyses, (ii) inviscid analyses with viscous corrections and (iii) fully viscous analyses. Although inviscid analyses (e.g. Refs. 1-6) can give accurate predictions of the blade pressure distribution in some cases, they are limited by their neglect of viscous phenomena which for some applications may be important. The limitations result from (i) the necessity of assuming airfoil circulation to obtain a unique flow field prediction, (ii) neglect of viscous displacement effects, and (iii) the inability to predict losses and heat transfer. Considering the first of these aspects, specification of the airfoil circulation may be both reasonable and straightforward for isolated sharp trailing edge airfoils at high Reynolds number operating below stall; in these cases the Kutta-Joukowski

---

1. Delaney, R. A. and P. Kavanagh: Transonic Flow Analysis in Axial-Flow Turbomachinery Cascades by a Time-Dependent Method of Characteristics. ASME Paper No. 75-GT-8, 1975.

2. Gopalakrishna, S. and R. Bozzola: A Numerical Technique for the Calculation of Transonic Flows in Turbomachinery Cascades. ASME Paper No. 71-GT42, 1971.

3. Ives, D. C. and J. F. Liutermoza: Analysis of Transonic Cascade Flows Using Conformal Mapping and Relaxation Techniques. AIAA Journal, Vol. 15, 1977, pp. 647-652.

4. Caspar, J. R., D. E. Hobbs and R. L. Davis: The Calculation of Two-Dimensional Compressible Potential Flow in Cascades Using Finite Area Techniques. AIAA Paper 79-0077, 1977.

5. Erdos, J. I., E. Alzner and W. McNally: Numerical Solution of Periodic Transonic Flow Through a Fan Stage. AIAA Paper 76-369, 1976.

6. Steger, J. L., T. H. Pulliam and R. V. Chima: An Implicit Finite Difference Code for Inviscid and Viscous Cascade Flow. AIAA Paper 80-1427, 1980.

condition, which requires the trailing edge point to be a stagnation point, has proved to be an effective tool in setting the airfoil circulation. However, proper specification of the circulation is not obvious for rounded trailing edge airfoils, such as those typically found in turbine cascades. Specification also remains a problem in time-dependent flows or in flows about blades having trailing edge separation. In all these cases, specification of the airfoil circulation may require use of an experimental data base.

Inviscid flow analyses also are limited by their neglect of viscous displacement effects. In cases where the boundary layer developing on the blade surface remains thin, flow field predictions neglecting boundary layer displacement effects may be quite accurate. However, if the boundary layer does not remain thin, the actual pressure distribution generated in the flow may be significantly affected by the boundary layer development. In these cases, the actual pressure distribution is often well represented by the inviscid pressure distribution about an equivalent body consisting of the physical body plus the viscous displacement surface. The viscous displacement effects will significantly alter the generated pressure field if the viscous displacement thickness becomes a significant fraction of the blade thickness, as is the case when boundary layer separation occurs. Even when viscous displacement effects are small, they may still be important and a particular example of such a situation occurs in transonic flow. In transonic flow the flow field is extremely sensitive to the effective airfoil shape, and an inviscid determination of the shock location may be unreliable unless the boundary layer thickness is very small. When the physical boundary layer viscous displacement effects change the effective airfoil geometry, an inviscid analysis prediction of shock location and strength may be significantly in error leading to a poor prediction of the entire flow field. A final problem associated with inviscid analyses is their inability to predict aerodynamic losses and heat transfer rates. If these quantities are desired, the inviscid analysis must be combined with some viscous correction procedure.

The need for including viscous phenomena in a cascade analysis has led to several approaches. One approach modifies the inviscid solutions for viscous effects via empirical data correlations or solves the boundary layer equations under the calculated inviscid pressure distribution. In regard to the first of these, although methods based upon data correlations can play a useful role in the design process, they are limited to flow conditions within the range of

correlating data. The second approach is considerably more general and a review of boundary layer techniques for turbomachinery applications has been presented by McDonald (Ref. 7). When the boundary layer remains thin throughout the flow, as it does in many practical applications, the combined inviscid flow-boundary layer analysis may give an adequate description of the flow even if viscous displacement effects on the pressure distribution are neglected. However, as previously discussed, in many practical applications severe pressure gradients, shock waves or transonic effects can cause significant displacement effects which in turn result in the actual pressure distribution being considerably different from that obtained via a purely inviscid analysis. In these situations an analysis which solves an inviscid set of equations to obtain a blade pressure distribution and then solves a set of blade boundary layer equations under the influence of this pressure distribution to account for viscous effects is inadequate, and a solution recognizing the mutual dependence of the pressure distribution and blade viscous effects is required. Two major approaches have been developed for such problems; these are the inviscid flow-boundary layer strong interaction analysis, and the fully viscous passage analysis. Rather than neglect the effect of viscous displacement upon the pressure field, boundary-layer strong-interaction analyses solve for both the nominally inviscid outer flow and the wall viscous layer in such a manner that viscous displacement effects are allowed to influence the generated pressure distribution. Typical strong interaction procedures can be found in Refs. 8-10.

A strong interaction analysis may take the form of either a forward-marching procedure or a global iteration. For regions where the inviscid flow

---

7. McDonald, H.: Computation of Turbomachinery Boundary Layers. The Aerothermodynamics of Aircraft Gas Turbine Engines. AFAPL-TR-78-52, 1978.

8. Levy, R., S. J. Shamroth, H. J. Gibeling and H. McDonald: A Study of the Turbulent Shock Wave Boundary Layer Interaction. Air Force Flight Dynamics Laboratory Report AFFDL-TR-76-163, 1976.

9. Klineberg, J. M. and L. Lees: Theory of Viscous-Inviscid Interactions in Supersonic Flow. AIAA Journal, Vol. 7, 1969.

10. Erdos, J., P. Baronti and S. Elszweig: Transonic Viscous Flow Around Lifting Two-Dimensional Airfoils. AIAA 5th Fluid and Plasma Dynamics Conference, AIAA No. 72-678, 1972.

is supersonic and thus described by hyperbolic equations, a solution can be forward-marched in space with the inviscid and viscous regions coupled on a station-by-station basis. The chief difficulty in this process is that mathematically stiff equations must be solved. Common problems with stiff equations show up in the form of numerical solutions which can quickly branch off the desired solution thus producing a physically unrealistic result. In regions where the inviscid flow is subsonic and thus described by elliptic equations, a forward-marching procedure without iteration is not physically realistic as a result of the upstream pressure propagation, and consequently a sequence of inviscid and boundary layer solutions must be performed in a manner where each stage corrects the former one through a global iteration. Additional problems occur in transonic cascades where mixed regions of flow are present and where small displacement effects may have considerable influence on shock location and overall pressure distribution. Further, if an interaction procedure is to be used, the viscous layer can be solved iteratively by either a forward-marching boundary layer calculation procedure or as the asymptotic condition of a time or pseudo-time dependent integration. In the case of steady state forward-marching boundary layer procedures, problems are encountered when the boundary layer is subjected to a strong enough adverse pressure gradient to cause separation. Although a boundary layer procedure can be forward marched through separation by suppressing streamwise convection terms in the separated flow region (the FLARE approximation) (Ref. 11), the resulting solution is based upon an approximation made in the separated flow region which becomes progressively more inaccurate as the backflow velocities increase. Therefore, calculated details of the flow in this region cannot be expected to be accurate with significant backflow using FLARE. A global, but time consuming, iteration is necessary to replace the FLARE approximation, and at this point the efficiency of the forward-marching scheme must be carefully evaluated to ensure a net gain exists relative to solving the full Navier-Stokes equations for the viscous layer. Time integration of the interaction between the boundary layer

---

11. Rehyner, T. and I. Flugge-Lotz: The Interaction of Shock Waves with a Laminar Boundary Layer. International Journal of Nonlinear Mechanics, Vol. 3, 1968.

and the external flow can be structured to avoid the use of either FLARE or the global iteration to account specifically for the backflow velocity (Ref. 12), and in some cases the time marched iteration approach may show a significant gain relative to solving the Navier-Stokes equations for the viscous flow region. However, the interaction approach remains limited, even with time integration, to flows where the division of the flow into zones which can be interacted is reasonable.

The second approach used in obtaining solutions for flows in which viscous phenomena significantly affect pressure distribution is the fully viscous analysis. The fully viscous analysis solves the entire flow field via a single set of equations, thus avoiding any need to divide the flow into viscous and inviscid regions. Two general approaches of this type for cascades have been used; one approach by Shamroth, Gibeling and McDonald (Ref. 13), is based upon the full ensemble averaged Navier-Stokes equations and a second approach based upon the so-called thin shear layer equations has been used by Steger, Pulliam and Chima (Ref. 6). The thin shear layer equations are an approximate form of the Navier-Stokes equations which contain all pressure and convective terms but retain only those viscous terms significant in thin shear layer flow aligned with one coordinate; the remaining viscous terms are omitted from the analysis. The fully viscous passage analyses overcome many of the problems associated with boundary layer strong interaction analyses as they avoid the need to divide the flow into viscous and inviscid regions and eliminate the iterative matching between regions. Furthermore, the full Navier-Stokes analysis contains all necessary convective, pressure and diffusion terms necessary to describe large separated regions correctly and, therefore, flows with significant separation or shear layers not aligned with one of the coordinates

---

12. Briley, W. R. and H. McDonald: Numerical Prediction of Incompressible Separation Bubbles. Journal of Fluid Mechanics, Vol. 69, 1975, pp. 631-635.

13. Shamroth, S. J., H. J. Gibeling and H. McDonald: A Navier-Stokes Solution for Laminar and Turbulent Flow Through a Cascade of Airfoils. AIAA Paper No. 80-1426, 1980.

present no special problem when the full set of equations is used. Furthermore, since fully viscous passage analyses are based upon time-dependent forms of the governing equations, these approaches can be used to study steady state flows, should they exist, as the asymptote of time integration and, in addition, these procedures can be used to study transient effects.

Demonstrations of thin shear layer calculations are presented in Ref. 6, and demonstrations of Navier-Stokes calculations are presented in Ref. 13. The results of Ref. 13 show that for this problem, the Linearized Block Implicit (LBI) procedure of Briley & McDonald (Ref. 14) was very efficient in solving the full Navier-Stokes equations, and converged pressure distributions for an unstaggered cascade of NACA 0012 airfoils were obtained in low Mach number laminar flow within sixty time steps. Turbulent flow calculations for the ensemble-averaged Navier-Stokes equations also converged within sixty time steps, with the calculation being initiated from a converged laminar solution. These very fast convergence rates demonstrate the practicality of applying Navier-Stokes analyses to the cascade problem. The results presented in Ref. 13 considered subsonic laminar and turbulent flow ($M_\infty \approx 0.15$) in a very simple cascade of unstaggered NACA0012 airfoils. The present report extends these results to transonic flow in a realistic cascade geometry. As a prelude to the transonic cascade calculation, it was deemed appropriate to consider a simple one-dimensional transonic flow and use this simple transonic test case to assess the role of type-dependent differencing, boundary conditions and artificial dissipation techniques. The present report discusses this assessment as well as extension of the constructive coordinate system generation process to include realistic cascade configurations. Finally, a sample high Reynolds number transonic calculation is presented.

---

14. Briley, W.R. and H. McDonald: Solution of the Miltidimensional Compressible Navier-Stokes Equations by a Generalized Implicit Method. J. Comp. Physics, Vol. 24, No. 4, August 1977, p. 372.

II NUMERICAL CONSIDERATIONS

Time-Marching and Iterative or Relaxation Procedures

To date both time-marching and iterative or relaxation solutions have been used to obtain steady solutions to transonic flow problems. In the time marching approach the governing unsteady equations are solved under the influence of steady state boundary conditions and a steady flow field, if it exists, may develop as the solution is marched in time (e.g. Refs. 13 - 15). In the relaxation approach the steady state form of the equations is considered and a converged solution, if it can be obtained, is achieved by first assuming values for the dependent variables throughout the flow field and then iteratively correcting or "relaxing" the assumed solution in a series of iterations until the governing steady state equations are satisfied (e.g. Refs. 16 - 19). Although each iterative correction or relaxation step can often be considered in some sense as a pseudo time step (e.g. Ref. 16), the time marching and iterative methods are not necessarily equivalent. One obvious difference concerns cases where no steady flow exists. In these cases an iterative or relaxation procedure, unless it can be formally related to the transient evolution, can at best only give some mean flow upon convergence and cannot predict the experimentally observed unsteady flow field. However, even in those cases where a steady flow exists, it should be recognized that the process by which an iterative or relaxation procedure reaches a steady solution need not (and, in general, does not) conform to any physical process. As a result, physical reasoning based upon

---

15. Magnus, R. and H. Yoshihara: Inviscid Transonic Flow Over Airfoils. AIAA Journal, Vol. 8, No. 12, pp. 2157-2162, 1970.

16. Murman, E.: Analysis of Embedded Shock Waves Calculated by Relaxation Methods. AIAA Journal, Vol. 12, 1974, p. 626.

17. Jameson, A.: Iterative Solution of Transonic Flows over Airfoils and Wings, Including Flows at Mach 1. Communications on Pure and Applied Mathematics, Vol. 27, 1974, p. 283.

18. Ballhaus, W. F., A. Jameson and J. Albert: Implicit Approximate Factorization Schemes for Steady Transonic Flow Problems. AIAA Journal, Vol. 16, June 1978, pp. 573-597.

19. Jameson, A.: Acceleration of Transonic Potential Flow Calculations on Arbitrary Meshes. AIAA Paper 79-1458.

actual flow processes may not be a valid guide in developing a convergent iterative procedure. The converse is also a possibility, that strategies and arguements developed from relaxation approach need not be required or useful in developing the transient approach. As a final introductory comment, it is useful to consider two subsets of time marching methods. In the first of these, no attempt is made to follow transients and as a consequence this subset may be thought of as a time consistent iterative approach to solve the steady flow equations. In the second subset, again no attempt is made to follow the transient but in addition the time step may be varied spatially and temporally to improve convergence. This is equivalent to a matrix conditioning (Ref. 20), but with the special constraint that the conditioning not change the type of the conditioned system and consequently the resulting iteration remains time consistent. For reasons that will be subsequently evident, the critical distinction between iterative and time consistent categories lies in the type of inferred equation system treated in the evolution process.

An example demonstrating these points can be found in the two-dimensional velocity potential equation. For unsteady flow, the two-dimensional velocity potential equation can be written as

$$\phi_{tt} + 2\phi_y\phi_{yt} + 2\phi_x\phi_{xt} = (a^2 - \phi_x^2)\,\phi_{xx} - 2\phi_x\phi_y\phi_{xy} + (a^2 - \phi_y^2)\,\phi_{yy} \qquad (1)$$

As can be demonstrated by a characteristic analysis, Eq. (1) is a second-order hyperbolic equation in the time variable, t. If the transient as well as the steady state solution of velocity potential is desired, it would be necessary to consider the time-dependent equation as represented by Eq. (1). However, if only the steady state solution is of interest, an iterative or relaxation procedure can be applied to the steady form of Eq. (2) which is obtained by setting time derivatives to zero

$$0 = (a^2 - \phi_x^2)\,\phi_{xx} - 2\phi_x\phi_y\phi_{xy} + (a^2 - \phi_y^2)\,\phi_{yy} \qquad (2)$$

When Eq. (2) is solved by a relaxation procedure, values are assumed for $\phi(x,y)$ at every grid point and the values are then corrected through a series of iterations until a steady state is reached. As a simple example, if a point relaxation based upon simultaneous displacement were used to solve the steady

two-dimensional potential equation, then ϕ^{n+1} would be related to ϕ^n by an equation of the form

$$D(\phi^{n+1}-\phi^n) = A\phi_{xx}{}^n + B\phi_{xy}{}^n + C\phi_{yy}{}^n + E(\phi_x^n, \phi_y^n, \phi^n) \tag{3}$$

where n is the iteration index, A, B, C and E are nonlinear coefficients and D is a function of the nonlinear coefficients, the spatial grid size and the relaxation parameter. If D is written instead as $1/\Delta\tau$ and $\Delta\tau = \phi^{n+1}-\phi^n$, the difference equation is a consistent approximation to the differential equation

$$\phi_\tau = A\phi_{xx} + B\phi_{xy} + C\phi_{yy} + E(\phi_x,\phi_y) \tag{4}$$

which, unlike the transient potential equation, is a parabolic differential equation of the first order in the marching direction τ. Equation (4) is termed the 'inferred differential equation' associated with the relaxation procedure. Obviously, this equation need not correspond to any physical transient process during its iterative development. For example, using a change of independent variables, Eq. (4), can be written in the form

$$\phi_\tau = A'\phi_{x'x'} + C'\phi_{y'y'} + E' \tag{4a}$$

Based upon experience with parabolic equations such as the heat conduction or diffusion equation, numerical difficulties may be expected (and have been experienced) if either A' or C' is negative. Further, based upon Eq. (2), negative diffusion is clearly a possibility depending on precisely how the iteration is set up, whenever the local velocity is supersonic. Any such negative diffusion in iteration space, if it were to occur, need have no physical relevance to the problem of interest. As a collorary, numerical strategies developed to counter the problem of negative numerical diffusion in interation space, need have no counterpart in the transient approach.

Although point relaxation with simultaneous displacement serves to demonstrate some differences between iterative and time-marching procedures, point relaxation is not a current method of solving transonic potential flow problems. Much more efficient methods have developed and are being used extensively which do not attempt to retain time consistency and are based upon successive line over-relaxation (Refs. 16 and 17) or alternating

direction implicit techniques (Refs. 18 and 19). A line relaxation procedure which solves the two-dimensional steady velocity potential equation using type-dependent rotated differences has been examined in detail by Jameson (Ref. 17). The resulting inferred differential equation is typical of these more efficient and more modern time inconsistent iterative schemes. As an example the inferred differential equation has [17] the principal part

$$(M^2-1)\phi_{ss} + 2\alpha\phi_{s\tau} - \phi_{nn} + 2\beta\phi_{n\tau} \tag{5}$$

where s is the streamwise direction, n is the direction normal to a streamline and τ is a pseudo-time variable representing the relaxation parameter. The coefficients α and β depend upon the relaxation parameter. Once again the differential equation inferred by the relaxation process does not represent the time-dependent velocity potential equation, and need not represent any physical process as it evolves. In order to elucidate Eq. (5), a new independent variable, T, is introduced

$$T = \tau - \frac{\alpha s}{M^2-1} + \beta n \tag{6}$$

which transforms the principal part to the form

$$(M^2-1)\phi_{ss} - \phi_{nn} - \left(\frac{\alpha^2}{M^2-1} - \beta^2\right)\phi_{TT} \tag{7}$$

The resulting equation, like the physical time-dependent equation, Eq. (1), and unlike the point relaxation equation, Eq. (4), contains second derivatives in the three dependent variables s, n and T. In subsonic flow (M<1), Eq. (7) is hyperbolic with T being the time-like coordinate and is of a similar type as the transient potential equation. In supersonic flow (M>1) the inferred differential equation remains hyperbolic, however, the time-like direction is no longer the independent variable T but rather is the independent variable s, the physical streamwise direction. It follows, therefore, that strategies required by these relaxation schemes to preserve stability when supersonic regions are encountered are not required a priori for the transient approach which does not change type upon encountering a supersonic region.

Although iterative and relaxation techniques have been very successful in obtaining inexpensive and accurate solutions for the transonic potential flow equation, several points should be emphasized. First, the inferred differential equation (or pseudo-time differential equation) actually being solved is not time consistent in supersonic flow. Secondly, the solution to this equation only represents the desired physical process when and if a steady solution to the equation is obtained. Finally, since the differential equation being solved does not correspond to a physical process during its transient phase, a physical knowledge of the actual flow process need not be relevant in developing a convergent solution procedure. Guidance for developing stable algorithms, boundary conditions, etc. must be obtained solely from the mathematical properties of the inferred differential equation, which in turn must be derived and analyzed. Unlike the iterative or relaxation methods, the methods which solve the physical unsteady equations model a physical problem during the transient flow process. Consequently, an understanding of both the flow physics and the mathematical properties of the equations can be used for guidance in choosing algorithms, boundary conditions, etc.

The foregoing discussion has served to demonstrate some of the broad similarities and differences between iterative and time-marching or time-consistent procedures. Both procedures have been used to solve transonic flow problems (Refs. 13 - 19) and in either case the key is to utilize a procedure which allows the efficient attainment of a stable steady solution consistent with the steady differential equation. Considering first the requirement of efficiency, the procedure should converge to the steady solution as quickly as possible so as to minimize computer run time. If it is desired to follow the physical transients, then a time-marching solution must be used with the time step chosen so as to obtain both stability and transient accuracy. However, if only the steady solution is of interest, then either a time-consistent solution or an iterative procedure can be used. However, it should be noted that if a time-marching procedure is utilized solely to obtain the steady solution, there is no need to follow the transient accurately. The only requirement is the rapid attainment of an accurate steady solution, and the time step may be as large as allowed by numerical stability considerations and, in fact, should be chosen to optimize the convergence rate. The experience of Shamroth, Gibeling and McDonald with subsonic flows (Ref. 13) has shown cascade flow fields to converge to steady state in approximately 60 time steps using a split

Linearized Block Implicit (LBI) (Ref. 14) scheme for the unsteady Navier-Stokes equations. As demonstrated subsequently in the present report and although no attempt has yet been made to accelerate the convergence rate for transonic cascade calculations for this flow, convergence is still obtained within 150 time steps.

In the past, the statement has frequently been made that iterative or relaxation schemes converge to the steady state more quickly than do time marching schemes. On the basis of the more recent studies (Ref. 14), including the present, it is clear that this statment applied to previous stability restricted explicit time-marching schemes, such as Ref. 15. This statement is not, at present, applicable to some of the current generation of implicit time-marching schemes. Further, it is also clear that rapid achievement of the steady state by a time-marching method results in, and perhaps even requires that, the transients not be resolved. When transients are not resolved the time-marching approach may be thought of as time-consistent iteration and as such retains the advantage that only the boundary conditions need distinguish between subsonic and supersonic flow. If the transients are not computed accurately, then the computed steady solution is subject to the same existence and uniqueness questions that the relaxation solutions are. The primary advantage of the time-marching or time-consistent approach is the ready ability to compute the transient flow, in addition to the steady flow, if required. This additional feature is obtained at little computational disadvantage, if any, compared to the current generation of iterative or relaxation approaches. It is also observed that the transient approach is straightforward to implement, and does not require special distinction in the interior flow between subsonic and supersonic regions. Boundary conditions are another matter, and in accordance with the flow of information as determined by the local characteristics, a distinction must be made between supersonic and subsonic flow on the boundaries.

It is noted that conditioning of the matrix which arises from an implicit time-dependent formulation can be used to accelerate convergence (Ref. 20). When this conditioning is restricted to premultiplication of the matrix equa-

---

20. McDonald, H. and W. R. Briley: Computational Fluid Dynamic Aspects of Internal Flows. AIAA Paper 79-1445.

tion by a positive diagonal matrix, the result is equivalent to taking a spatially varying time step and the scheme remains time consistent. It is readily apparent that such a procedure will scale the slope of the characteristics in time, but leaves both the sign and the eventual steady flow unaltered. Such a conditioning thus leaves the type of the governing equations unchanged, together with the boundary conditions. Hence, this scaling retains the attributes of the transient approach, but with improved convergence, while retaining the ability to perform accurate transient calculations by simply preconditioning with the unit matrix.

Spatial Differences, Boundary Conditions and Artificial Dissipation

The previous favorable experience obtained in applying the LBI procedure of Ref. 14 to subsonic cascade flow fields (Ref. 13) in conjunction with the considerations of the previous subsection argue strongly for applying this same technique to the transonic cascade problem. However, prior to this application several items must be considered. These include spatial differencing, boundary conditions and artificial dissipation. Obviously, these items are strongly connected and cannot be considered independently. For example, some spatial difference schemes contain a dissipative truncation error which is equivalent to an implicit artificial dissipation. Also the type of spatial differencing chosen will affect the number of boundary conditions required to close the algebraic set of difference equations.

Previous investigators of transonic flow problems with some exceptions (e.g. Ref. 15) have concentrated primarily upon solutions of the potential flow equations. Their analyses have used a variety of combinations for spatial differencing, boundary conditions and artificial dissipation. The present approach focuses upon the full ensemble-averaged, time-dependent Navier-Stokes equations, thus including both rotational and viscous effects. The analysis applies a split LBI algorithm to the governing equations, expresses spatial derivatives via central differences throughout the flow and selectively adds an explicit artificial dissipation term to the equations. As shall be demonstrated subsequently, when this procedure is used with careful attention paid to boundary conditions, it leads to rapid convergence and sharp representation of the transonic shock. Prior to consideration of the Navier-Stokes cascade calculation, the problems of boundary conditions, spatial differences and artificial dissipation were investigated through a one-dimensional transonic model problem.

Model Problem for Transonic Flow

A simple model problem consisting of one-dimensional flow with specified heat sources is used to examine techniques for treating spatial differencing, boundary conditions and artificial dissipation. The equations solved are the continuity equation

$$\frac{\partial \rho}{\partial t} + \frac{\partial \rho u}{\partial x} = 0 \tag{8}$$

the momentum equation

$$\frac{\partial \rho u}{\partial t} + \frac{\partial \rho u^2}{\partial x} - \frac{\partial p}{\partial x} = \frac{\partial \tau_{xx}}{\partial x} \tag{9}$$

and the energy equation

$$\frac{\partial \rho C_p T^o}{\partial t} + \frac{\partial \rho u C_p T^o}{\partial x} = \frac{\partial p}{\partial t} + \frac{\partial [u\tau]}{\partial x} - \frac{\partial}{\partial x} k \frac{\partial (T^o - u^2/2C_p)}{\partial x} + q(x) \tag{10}$$

where ρ is density, u is velocity, p is pressure, C_p is specific heat, T^o is total temperature, τ is shear stress, q is a heat source, t is time and x is the spatial coordinate. In one-dimensional flow, acceleration or deceleration can be obtained by varying the heat source-sink distribution $q(x)$. At subsonic Mach numbers, a heat source ($q>0$) accelerates the flow while a heat ($q<0$) sink decelerates the flow; at supersonic Mach numbers the effects are reversed with heat addition leading to deceleration and heat removal leading to acceleration (cf. Ref. 21). By an appropriate selection of Mach number, Reynolds number and heat source-sink distribution, this model problem permits study of a wide range of flow conditions including subsonic, supersonic and transonic flow with and without discontinuities.

---

21. Shapiro, A.: The Dynamics and Thermodynamics of Compressible Fluid Flow. Rowland Press, New York, 1958.

In considering the boundary condition problem, guidance can be obtained from a characteristics analysis of the inviscid equations. The characteristics analysis reveals how boundary data is propagated into the solution domain by the differential equations and thus can be used to determine how boundary conditions should be chosen for an inviscid flow solution procedure. The number of boundary conditions required at any boundary point is equal to the number of characteristics originating at the point which transfer information from the boundary point into the interior flow field. Thus, the characteristics analysis determines the number of boundary conditions to be applied to each boundary point, but does not specify particular boundary condition equations. The inviscid characteristics analysis shows that two boundary conditions are required at a subsonic inflow boundary, one boundary condition is required at a subsonic outflow boundary, three boundary conditions are required at a supersonic inflow boundary and zero boundary conditions are required at a supersonic outflow boundary.

Although these boundary conditions would suffice for a characteristics solution, the situation becomes more complicated when a finite difference method is used to solve the equation set. If, as in the present calculation, central spatial differences are used to represent spatial derivatives and the equations are written at each interior point, then three conditions must be written at each boundary point to complete the resulting set of algebraic equations. As indicated by the characteristics analysis, the differential equations allow specification of three conditions; the remaining three conditions required to close the set of equations result solely from the use of central differences and they are termed extraneous conditions. These extraneous boundary conditions must be consistent with the physical flow situation or spurious numerical solutions may result. These concepts regarding boundary condition specification are tested subsequently by solving simple problems. In the test calculations which follow, temporal derivatives are represented by first-order backward time differences and spatial derivatives are represented by second-order accurate central differences. Following Briley and McDonald (Ref. 14) the equations are solved by a Linearized Block Implicit (LBI) scheme where nonlinear terms are linearized by Taylor series expansion about the solution at a known time level and the equations are solved as a coupled set. Details of the procedure are given in Ref. 14.

The boundary condition test case for use with central spatial differences is first explored for one-dimensional subsonic and supersonic uniform flows at a Reynolds number, Re_ℓ, of approximately 2.2×10^7. The quantity Re_ℓ is the Reynolds number of the problem defined as $Re_\ell = \rho u \ell / \mu$ where ρ, u, μ are free stream density, velocity and viscosity respectively and ℓ is the domain length. The cell Reynolds number, $Re_{\Delta x}$, in these cases was of the order 10^6 where $Re_{\Delta x} = \rho u \Delta x / \mu$ and Δx is the grid spacing. Central difference solutions may develop spatial oscillations at high cell Reynolds numbers unless artificial dissipation is added to the equations either explicitly (by the addition of a dissipation-like term) or implicitly (e.g., one-sided differencing). For certain model problems representing a balance of convection and normal diffusion (Ref. 22), the maximum cell Reynolds number which can be obtained without the appearance of spatial oscillations is 2, and many numerical procedures require some artificial dissipation if the cell Reynolds number for the problem being solved and grid being used is above this value. This point will be considered in some detail subsequently when artificial dissipation is discussed. The equations solved were the continuity equation, the momentum equation and the energy equation with $q = 0$. A nonuniform distribution of the dependent variables was specified at time $t = 0$ and the solution marched in time; the exact solution at large times is uniform flow with constant ρ, u, T^o.

As discussed previously, the characteristics analysis shows that for subsonic flow two conditions must be specified on the inflow boundary and one on the outflow boundary. With this as a guide, total temperature and total pressure were specified on the inflow boundary and static pressure was specified on the outflow boundary. Since spatial derivatives are represented by central differences, three extraneous boundary conditions are required. For these cases the second derivative of density was set to zero on the inflow boundary, and second derivatives of velocity and total temperature were set to zero on the

---

22. Roache, P. J.: Computational Fluid Dynamics. Hermosa Press, Albequerque, 1972.

downstream boundary. This set of boundary conditions is referred to as subsonic-subsonic. It should be noted that the specified extraneous conditions are consistent with the exact solution. Additional cases were run with boundary conditions chosen for supersonic flow. In these cases total temperature, velocity, and density were specified at the inflow boundary and the second derivatives of these quantities were set to zero at the outflow boundary. This set of conditions is termed supersonic-supersonic. Although viscous equations are solved in this test case, a high Reynolds number is considered and the flow behavior is essentially inviscid. Therefore, the guidance obtained from the inviscid characteristics analysis would be expected to be valid. The four cases studied are given in TABLE I

TABLE I - UNIFORM FLOW CASES

Case	M	Boundary Conditions
1	<1	Subsonic - Subsonic
2	<1	Supersonic - Supersonic
3	>1	Subsonic - Subsonic
4	>1	Supersonic - Supersonic

The test cases were initiated as nonuniform flows, all subsonic or all supersonic, as the case might be, which satisfied the boundary conditions, and then the flow was allowed to develop in time. Although the calculations were run at a high cell Reynolds number using spatial central differences with no artificial dissipation term added for numerical stability, the entirely subsonic flow case with subsonic-subsonic boundary conditions and the entirely supersonic flow case with supersonic-supersonic boundary conditions converged rapidly to the exact uniform solution. However, both the subsonic flow run with supersonic-supersonic boundary conditions and the supersonic flow run with subsonic-subsonic boundary conditions developed severe spatial oscillations and failed to converge. The two convergent calculations were repeated with initial conditions specified which did not satisfy the zero derivative boundary conditions. The discrepancy between the initial flow and the specified boundary conditions did not hinder convergence.

These test calculations demonstrate that converged solutions can be obtained for both subsonic and supersonic uniform flow using central spatial differences in each case, provided boundary conditions are treated adequately. One-sided or retarded differences were not required to obtain a converged supersonic flow solution. These boundary conditions used in the converged calculations are consistent with an inviscid characteristics analysis and employ exact extraneous boundary conditions. No explicit or implicit artificial dissipation was required in this simple case of unidirectional flow which is uniform in the steady state.

Nonuniform Subsonic Flow

Further test calculations were made for one-dimensional nonuniform subsonic flow. As in the subsonic uniform flow case, total temperature and total pressure were set as upstream boundary conditions and the density gradient at the upstream boundary was set to zero. The downstream boundary conditions consisted of specified static pressure and zero derivatives of velocity and total temperature. The flow was accelerated by specifications of a heat source distribution in the energy equation, Eq. (10); however, the heat sources at both ends of the domain were brought smoothly to zero so as to be consistent with the zero gradient boundary conditions used. A dependent variable distribution was assumed for an initial flow field and the solution allowed to develop in time. With the specified heat distribution, the solution converged and upon convergence the values of the dependent variables at the upstream boundary were

$$W_1 = 1.1062\ W_{ref}$$

$$P_1 = .9898\ P_{ref}$$

$$T_1^o = 1.0166\ T_{ref}^o$$

where W is axial velocity, P is pressure and T^o is total temperature. The exit conditions for an inviscid Rayleigh solution with the above inlet conditions and the same specified heat source distribution are compared to the computed $Re = 10^6$ solution in Table II.

TABLE II - NONUNIFORM SUBSONIC FLOW

	Rayleigh solution	Present solution
W_2	1.2004	1.2000
P_2	.9771	.9774
T_2^o	1.0919	1.0938

As can be seen, the numerical solution at high Reynolds number is in excellent agreement with the inviscid Rayleigh solution, and despite the very high cell Reynolds number convergence was obtained readily without significant spatial oscillations using central spatial differences and with no artificial dissipation.

Mixed Subsonic-Supersonic Flow

The next flow situation investigated was characterized by positive heat sources in the upstream region of the flow and negative heat sources (heat sinks) in the downstream region. A continuous initial flow condition which contained subsonic flow in the region of the heat sources and supersonic flow in the region of the heat sinks was chosen. Upstream boundary conditions of specified total pressure, specified total temperature and zero density derivative were set; as determined earlier these conditions appear adequate for a subsonic inflow boundary. The downstream boundary conditions specified zero gradient for all three dependent variables, velocity, density and total temperature; as determined earlier these conditions are consistent with the exact solution. Thus, for the mixed flow problem both inflow and outflow boundary conditions were set consistent with an inviscid characteristics analysis with extraneous conditions set to be consistent with the exact solution. The Reynolds number was set at 10^6, and the solution was then allowed to develop with time.

The solution first approached a flow field consistent with an inviscid Rayleigh solution having a throat at the location where the heat sources changed from positive to negative values. During this portion of the calculation, the change in the dependent variables across a time step became less than one percent, with the time step being the time required for a particle traveling at sonic velocity to pass from one grid point to another. However, the calculation was allowed to continue and the solution began to diverge with an "expansion shock" appearing across the sonic region. The difference equations across the shock satisfied the momentum and continuity equations with a T^o change consistent with the heat source. Thus, the solution shifted abruptly from the subsonic branch of the Rayleigh curve to the supersonic branch of the Rayleigh curve. This solution represents a physically unrealizable flow field (e.g. Ref. 21). As the calculation continued, the strength of the expansion shock increased with the subsonic region being driven towards stagnation conditions and the supersonic region being driven toward very high Mach numbers. Convergence of this solution to a steady state did not appear possible and the solution was discontinued. It appeared that without something akin to artificial dissipation a solution could not be obtained at this Reynolds number with the boundary conditions taken from the inviscid characteristics analysis.

Test Calculations with Artificial Dissipation

Second Order Dissipation

The "expansion shock" discussed in the previous section is likely to occur only at high Reynolds numbers. If large viscous terms were present, they would tend to dissipate the discontinuous flow region. Two general methods exist for adding nonphysical dissipative mechanisms to the equations. In the first method, the truncation error associated with the spatial difference representation represents a dissipative type term. An example of this approach is the retarded difference representation (e.g. Ref. 16). In the second general method, dissipation is added explicitly through an additional term. Since the present approach utilizes spatial central differences which do not have a dissipative type truncation error associated with them, the present approach utilizes an explicit artificial dissipation whose magnitude can be precisely controlled.

Several different methods of adding artificial dissipative terms have been proposed, and all attempt to add dissipative phenomena only in regions of the flow where the artificial terms are required either for numerical stability or to suppress the short wavelength oscillations generated by the discontinuity. Three commonly used artificial dissipation devices are second-order dissipation (artificial viscosity), fourth-order dissipation and dissipation coefficient based upon pressure derivative. In second-order dissipation, a second-order term of the form $\alpha_2 \partial^2 \phi / \partial x^2$ is added to the governing equation where α is a dissipation coefficient and ϕ is a flow variable. As usually applied, fourth-order dissipation adds an entirely new type of term to the governing equations, of the form $- \alpha \partial^4 \phi / \partial x^4$. In the final type of artificial dissipation considered, the additional dissipative term is made proportional to the second derivative of pressure. In all cases, the question arises as to whether the addition of the artificial dissipation terms would destroy the essential features of solutions which contain very rapid unresolved spatial changes in the dependent variables. Therefore, a study of the effect of adding artificial dissipation to the governing set of equations was made.

In pursuing this study and considering the results which will be presented, several items should be kept in mind. First of all, the one-dimensional problem which serves as the test problem represents a balance between convective and streamwise diffusive phenomena. These are the important phenomena in shock flow considerations, but these are not the dominant phenomena in other important applications such as shock-free regions of shear flow where transverse diffusion may be critical. Secondly, the equations are being solved by an LBI method (Ref. 14) with second-order accurate central differencing used throughout. Thus, (except for the negligible axial diffusion due to viscous terms in this 10^6 Reynolds number flow) the artificial viscous terms represent the only dissipative terms present. Other methods may contain more or less spatial dissipation due to truncation error which could be of higher or lower order and, therefore, other solution procedures might behave differently. Finally, the present analysis utilizes density, velocity and total temperature as dependent variables. Other procedures may choose alternate sets of dependent variables, with consequent changes in the observed effect of the artificial dissipation.

In the second-order artificial dissipation formulation, the dissipative terms

$$\frac{d_1}{\rho}\frac{\partial^2 \rho}{\partial x^2}, \quad d_1 \frac{\partial^2 u}{\partial x^2}, \quad d_2 \frac{\partial^2 T^o}{\partial x^2}$$

are added to the right-hand sides of Eqs. (8), (9), and (10) respectively. The question arises as to the choice of values for d_1 and d_2. For the purpose of the discussion a dissipation parameter σ is defined by

$$\frac{\rho u \Delta x}{(\mu + d_1)} \leq \frac{1}{\sigma}$$

$$\frac{\rho u C_p \Delta x}{(k + d_2)} \leq \frac{1}{\sigma} \tag{11a}$$

or equivalently

$$d_1 \geq \sigma \rho u \Delta x - \mu$$

$$d_2 \geq \sigma \rho u C_p \Delta x - k \tag{11b}$$

In the second-order dissipation formulation a value is chosen for the dissipation parameter, σ, and this choice leads to a field specification of d_1 and d_2 with the stipulation that neither be negative. High values of σ imply relatively large artificial dissipation terms and low values imply relatively small artificial dissipation terms.

The subsonic-inflow supersonic-outflow case described previously then was recalculated with the artificial dissipation terms included for a series of dissipation parameters. As shown in Fig. 1, the calculation made with a dissipation parameter value of .5 was severely damped and differed significantly from the inviscid Rayleigh solution. It is believed that in view of the physical Reynolds number of 10^6 there should be little difference between the Rayleigh solution and an accurate numerical solution. When an σ = .025 condition was imposed, the calculated solution agreed very well with the inviscid solution. The last case considered set σ at a value of .0025 and although convergence was obtained, a physically unrealistic "expansion shock" similar to that obtained earlier without any artificial dissipation terms present was predicted at the throat. Thus, the results of Fig. 1 inidcate that, for the simple case

presented, an artificial viscosity formulation can give physically realistic results with a suitable choice of dissipation parameter. When the dissipation parameter is set to 0.5, the results are smeared so that they significantly differ from the desired inviscid solution. However, at lower values of the dissipation parameter, $\sigma = .025$, a solution which shows good agreement with the known inviscid solution is obtained and finally, at the lowest dissipation parameter investigated, $\sigma = .0025$, a physically unrealistic discontinuity appears in the solution. When considering the results of this test calculation, it should be emphasized that the model problem is dominated by a balance between convective, pressure and streamwise diffusion terms. It does not address the shock-free shear layer problem where the balance is dominated by convective, pressure and transverse diffusion terms.

A different flow situation can be obtained with the same distribution of heat sources and sinks by imposing a downstream static pressure boundary condition. However, once the total temperature and static pressure at the sonic throat are determined, and if the heat source distribution downstream of the throat is specified, then the Rayleigh solution admits only two possible exit pressures. The first is the supersonic pressure shown in Fig. 1; the second is a subsonic pressure which occurs when a shock is present at any location between the throat and the downstream boundary. Unlike the case of flow in a nozzle where the nozzle exit pressure varies with the shock position, the Rayleigh line solution gives the same downstream pressure for all shock locations.

For the conditions of the model problem the permissible downstream subsonic pressure is 1.19 times the static pressure at the throat, p^* (Ref. 21). A dissipation parameter study was made for one-dimensional flow with the pressure at the downstream boundary being $1.19p^*$, and the results are shown in Fig. 2. The calculation made for $\sigma = .025$ predicted a shock to occur when the flow encountered an adverse pressure gradient. The shock was spread over three grid points and except for a small post-shock overshoot, the results compared favorably with a Rayleigh line calculation that contains a shock at the same location. The $\sigma = .025$ calculation converged over most of the flow field; however, at the end of the run temporal changes (oscillations) were still occurring in the immediate vicinity of the shock. The calculation with $\sigma = .5$ once again converged but showed a considerable discrepancy with the inviscid solution as a result of excess dissipation. In fact, the $\sigma = .5$ solution did not even contain a super-

sonic region. Finally, the $\sigma = .0025$ calculation became unstable as a large preshock overshoot occurred and the calculation would not converge.

Since only two downstream static pressures are permissible when the inviscid flow is sonic at the throat, it is instructive to examine the results of calculations made at high Reynolds numbers when downstream boundary conditions inconsistent with the inviscid flow are specified. Figure 3 shows the results of calculations made when the downstream pressure is set at $0.812p^*$; this downstream pressure is lower than the permissible inviscid supersonic value. The $\sigma = .5$ calculation proceeds smoothly into this boundary condition through a sudden acceleration in the downstream portion of the calculation region. The $\sigma = .025$ calculation shows severe spatial oscillations and although the calculation does not appear to diverge, the calculation would not converge to a steady state in the allotted time. The results of a calculation made for $P_b = p^*$ are shown in Fig. 4. This value of back pressure is between permissible subsonic and supersonic values and again represents a physically unrealizable inviscid flow. Once again the $\sigma = .5$ calculation appears smooth and satisfies the boundary condition. However, the $\sigma = .025$ calculation shows severe spatial oscillations and although once again it did not diverge, it did not achieve steady state. Thus, for this simple flow the $\sigma = .5$ criterion accepts the imposition of physically unrealistic inviscid boundary conditions without exhibiting any obvious inconsistent behavior.

Fourth-Order Dissipation

The second-order dissipation approach represents one technique for adding artificial dissipation to the system of viscous flow equations; however, it represents only one of several methods which have been suggested. One alternative method is the fourth-order dissipation approach where the term $(-\alpha_4 \partial^4 \phi/\partial x^4)$ is added to the right-hand sides of the equations; ϕ represents ρ, u, T^o for the continuity, momentum and energy equations, respectively. Such an approach has been used by several investigators (e.g. Ref. 23) sometimes in conjunction

---

23. Beam, R. M. and R. F. Warming: An Implicit Factored Scheme for the Compressible Navier-Stokes Eqs. Proceedings of AIAA Third Computational Fluid Mechanics Conference, 1977.

with second-order dissipation. In some approaches the coefficient α_4 is a function of the time step (e.g., Ref. 23); however, if α_4 is a function of the time step, the steady state finally reached will be dependent upon the time step used in the calculation; therefore, α_4 was made independent of time step in the present investigation. There are two general methods of including fourth-order dissipation in the numerical procedure. In the implicit treatment, the size of the matrix being inverted increases from a block tridiagonal to a block pentadiagonal form and the cost of matrix inversion more than doubles. This large increase in the matrix inversion time is difficult to justify on the basis of artificial dissipation alone and, therefore, the implicit inclusion of fourth-order dissipation was not considered further. The second method considered includes the additional terms in the difference equations in an explicit manner. Since this does not increase the computer run time by any significant amount, this explicit approach was evaluated. The one-dimensional shock calculation was made for three different values of α_4, α_4 = 0.03, 0.20, 1.0. In all cases the calculation included an insignificant amount of second-order dissipation with σ held at .00025. When the smallest value of α_4 was used, α_4 = 0.03, the resulting calculation did not converge, and contained both a large "expansion shock" near the throat and a large compression shock near the downstream boundary. The calculation made using the large value of α_4 = 1, also gave very poor results as it developed large diverging spatial and temporal oscillations. This adverse behavior shown by the large α_4 calculation may be related to violation of an effective explicit stability limit associated with the explicit representation of the dissipation term.

The final fourth-order dissipation case considered was run with α_4 = 0.20. The results of this calculation are shown in Fig. 5. As can be seen in Fig. 5, the results are not very different from the second-order σ = .025 case, the solution was unchanging over most of the flow field but at the end of the run some temporal changes were still occurring in the vicinity of the shock.

Pressure Derivative Damping Coefficient

The final approach considered follows the 'shock smearing' technique used in Ref. 24 and adds the term $\alpha_4(\Delta x)^3(|u|+c)/4p\ \partial^2 p/\partial x^2 \partial^2 \phi/\partial x^2$ to the right-hand side of each equation. The factor $\alpha_4(\Delta x)^3(|u|+c)/4p\ \partial^2 p/\partial x^2$ may be interpreted

as a viscous diffusion coefficient whose strength depends upon the local pressure gradient. Viewed in this manner the additional term may be looked upon as a quasilinear second-order term, which can be treated implicitly. Two calculations were run with this formulation; the first assumed $\alpha_4 = 0.0005$ and the second set α_4 at 0.02. In the $\alpha_4 = 0.005$ calculation, steady state was never obtained, as the calculation developed strong spatial oscillations which varied with time. The second calculation made for $\alpha_4 = 0.02$ appeared much smoother; however, the predicted shock was smeared considerably more than the $\sigma = .025$ second-order dissipation calculation.

Mass Flux Damping

The test cases presented in Figs. 1 - 6 all consider the dependent variables to be ρ, u, T^o, however, another possibility is to choose ρ, ρu, and T^o as dependent variables. In this latter case the artificial dissipation terms are constructed so as to suppress the short wavelength spatial oscillations in the quantities ρ, ρu, and T^o. For the case of second order dissipation this consists of adding terms

$$\frac{d_1}{\rho}\frac{\partial^2 \rho}{\partial x^2}, \quad \frac{d_1}{\rho}\frac{\partial^2 \rho u}{\partial x^2}, \quad d_2 \frac{\partial^2 T^o}{\partial x^2}$$

to the governing equations with d_1 and d_2 being chosen so as to satisfy a dissipation parameter criterion. This set of artificial dissipation quantities is termed SET B whereas the original set based upon the terms

$$\frac{d_1}{\rho}\frac{\partial^2 \rho}{\partial x^2}, \quad d_1 \frac{\partial^2 u}{\partial x^2}, \quad d_2 \frac{\partial^2 T^o}{\partial x^2}$$

is termed SET A. Results of the 'SET B' artificial dissipation formulation along with a Rayleigh line solution are presented in Fig. 7 for three values of dissipation parameter. As shown in Fig. 7, the solutions for σ of .5 and .1 both contain excessive damping as neither properly represents the shock region. The results for $\sigma = .05$ shows better agreement with the Rayleigh solution, however, the computed solution contains relatively strong spatial oscillations. A comparison of 'SET A' and 'SET B' damping formulations for dissipation

parameters of .05 and .025 are shown in Figs. 8 and 9. As can be seen from these figures, a better numerical representation of the problem appears to result from the 'SET A' artificial dissipation formulation (ρ, u, T^o) at σ = .025.

Summary

This one-dimensional model problem has served to focus upon properties of artificial dissipation techniques which are relevant to the transonic shock flow field. The problem itself represents a case where the flow field equations are balanced by convective-pressure and axial diffusion phenomena. As in the transonic cascade, the shock results from the specification of a downstream static pressure condition and, therefore, the mechanism for shock generation in the transonic cascade problem of interest and in the one-dimensional model problem are very similar. With these considerations in mind, results of the model problem analysis can give guidance to the transonic cascade shock capturing problem.

The numerical results for the model problem can be assessed by comparison to one-dimensional inviscid theory for flow with heat sources. Although this Rayleigh solution is not unique in terms of the shock position, once this position is specified, the analytic solution can be used to evaluate the artificial dissipation models. For (i) the solution procedure used and (ii) the problem considered, second-order dissipation with a dissipation parameter, σ, equal to 0.025, gives very good agreement with the 'shocked Rayleigh solution'. Obviously, extrapolation of these results to the complicated two-dimensional transonic cascade problem must be somewhat speculative. However, since the shock in the transonic case is aligned fairly closely with a coordinate line, it is reasonable to expect that an accurate shock capturing procedure could be obtained by adding second-order artificial dissipation to the governing equations with the dissipation parameter taken to be the order of 0.025.

III. CASCADE ANALYSIS

Coordinate System

With increasing development of computational techniques many of the procedures originally developed to solve viscous flow equations in simple coordinate systems are being applied to realistic geometric configurations. Such applications require the development of suitable computational coordinate systems. For a coordinate system to be computationally suitable it must satisfy conditions of (i) generality, (ii) smoothness, (iii) resolvability and (iv) allow easy implementation of boundary conditions. Considering these conditions one by one, a coordinate generation technique should be fairly general allowing specification of airfoil shapes and cascade configurations of practical interest. Secondly, the technique must generate coordinate systems sufficiently smooth to allow reliable, accurate calculations. This requirement is more stringent than simply requiring the existence of a given number of coordinate transformation derivatives; the coordinates must not have large changes in the coordinate geometry data between grid points for, if large changes exist, the solution accuracy will deteriorate. An assessment of the smoothness requires a detailed examination of the metric data. Concerning the third requirement, the grid generation technique must allow high grid resolution in specified regions of the flow field. For example, the wall region of viscous flows is characterized by rapid changes in flow variables. Therefore, the computational grid should have a large number of points in the viscous wall region. Other regions in the flow are regions of slow changes in flow variables and these regions should have a relatively sparse computational grid associated with them. Finally, the technique must allow accurate specification of the required boundary conditions. If flow on a given line is to satisfy a no-slip condition, then it is important that this no-slip line be a coordinate line. The specification of boundary conditions on a boundary line which is not a coordinate line may present a difficult problem for Navier-Stokes analyses. Although finite difference molecules can be constructed for boundary points which do not fall upon coordinate lines, such molecules may have an unacceptable truncation error associated with them. Further, it should be noted that the boundary condition problem arises in both viscous and inviscid analyses; however, the problem is considerably more severe in viscous flows where no-slip conditions on solid walls can combine with boundary condition truncation error to produce numerical

solutions which are both qualitatively and quantitatively in error. Similarly, if a given line is a periodic line, it is also important that the periodic line be a coordinate line since boundary conditions are applied here. In addition, application of the periodic condition is greatly facilitated if the coordinate metric data is continuous across the periodic line. If the generated metric coefficients are discontinuous across periodic lines, a device such as one-sided differencing would be required to represent the equations at this location with a consequent loss of accuracy.

Among the coordinate system generation techniques currently used are conformal mapping techniques, techniques based upon a solution of Poisson's equation and constructive techniques. An example of a conformal mapping technique applied to the cascade problem is given by Ives and Liutermoza (Ref. 3). Examples of coordinate systems generated by the solution of a Poisson equation can be found in the work of Thompson and his coworkers (e.g. Ref. 25) or Steger and Sorenson (Ref. 26). The third approach to the coordinate system problem is the constructive approach used by Gibeling, Shamroth and Eiseman (Ref. 27) for the isolated airfoil problem and by Eiseman (Refs. 28 and 29) for the cascade problem. Application to the isolated airfoil problem is discussed by Shamroth and Levy (Ref. 30) and a description of its application to the cascade problem is discussed by Shamroth, Gibeling and McDonald (Ref. 13).

---

25. Thompson, J. F., F. C. Thames and C. W. Mastin: Boundary Fitted Curvilinear Coordinate Systems for Solution of Partial Differential Equations on Fields Containing Any Number of Arbitrary Two-Dimensional Bodies. NASA CR-2729, July 1977.

26. Steger, J. L. and R. L. Sorenson: Automatic Mesh Point Clustering Near a Boundary in Grid Generation with Elliptic Partial Differential Equations. Journal of Computational Physics, Vol. 33, 1979, p. 405.

27. Gibeling, H. J., S. J. Shamroth and P. R. Eiseman: Analysis of Strong-Interaction Dynamic Stall for Laminar Flow on Airfoils. NASA CR-2969, April 1978.

28. Eiseman, P. R.: A Coordinate System for a Viscous Transonic Cascade Analysis. United Technologies Research Center Report R76-912149-4, 1976.

29. Eiseman, P. R.: A Coordinate System for a Viscous Transonic Cascade Analysis. J. Comp. Physics, Vol. 26, March 1978, pp. 307-338.

30. Shamroth, S. J. and R. Levy: Description of a Constructive Coordinate System Generation Computer Code for Airfoils. SRA Rpt. R80-1, 1980.

Although the analysis described in Ref. 13 in principle could be used for a cascade of arbitrary airfoils, the coordinate generation code was limited to unstaggered cascades of symmetric, uncambered airfoils. The code has been generalized by Kim and Shamroth (Ref. 31) to allow specification of more arbitrary airfoil cascades and it is this generalized analysis which was used in the present effort.

In brief, the constructed coordinates are still obtained from the four loop system described in Ref. 13. However, with the generalization described in Ref. 31, the outer loop follows the camber line over the covered portion of the cascade and the blade surface itself is input via discrete data points. In addition, the coordinate orthogonality condition at the airfoil surface has been relieved in the vicinity of the airfoil leading edge and in this region the strict orthogonality condition has been replaced by the requirement of a smooth variation in the coordinate angle.

A plot of the coordinate system used in the cascade calculations of the present report is shown in Fig. 10 where the calculation utilized a 30 x 113 grid. The actual inner curve representing the airfoil is a smooth curve defined by 500 specification points. Only selected coordinate lines are shown on this plot with pseudo-radial coordinate lines in the vicinity of the leading edge and pseudo-azimuthal lines in the vicinity of the airfoil leading edge being omitted for clarity. To resolve the turbulent boundary layer viscous sublayer grid pseudo-radial spacing in the immediate vicinity of the blade was .00004 chords. The pseudo-azimuthal spacing in the vicinity of the blade leading edge is 0.0046 chords, as resolution of the suction peak was believed to be a critical factor for the streamwise mesh. In addition, the grid extends until two chords downstream of the blade trailing edge.

The Governing Equations

A sufficient set of governing equations to solve the viscous cascade problem for the flow conditions of interest is the ensemble averaged Navier-Stokes equations along with the usual continuity equation and an energy equation. However, there still remain decisions to be made on the choice of

---

31. Kim, Y. N. and S. J. Shamroth: Revised Coordinate Generation Program for a Cascade of Arbitrarily Shaped Airfoils. SRA Rpt. 81-1, 1981.

dependent variables and the precise form of these equations. The problem is further complicated by the presence of a complex geometry. Many previous Navier-Stokes analyses have concentrated upon flows in Cartesian or cylindrical geometries and in these cases the form of equations is considerably simpler than the form which occurs in the general case. The presence of complex geometries has required a reevaluation of the choice of equation form and dependent variables, and such a reevaluation has been made by Shamroth and Gibeling (Ref. 13). As a result of the reevaluation, Ref. 13 suggests the governing equations be transformed from the Cartesian coordinates x,y to a new set of coordinates ξ,η, where

$$\xi = \xi(x,y,t)$$

$$\eta = \eta(x,y,t) \tag{13}$$

$$\tau = t$$

and then written as

$$\frac{\partial W}{\partial \tau} + \xi_t \frac{\partial W}{\partial \xi} + \xi_x \frac{\partial F}{\partial \xi} + \xi_y \frac{\partial G}{\partial \xi} + \eta_t \frac{\partial W}{\partial \eta} + \eta_x \frac{\partial F}{\partial \eta} + \eta_y \frac{\partial G}{\partial \eta}$$
$$= \frac{1}{Re}\left[\xi_x \frac{\partial F_1}{\partial \xi} + \eta_x \frac{\partial F_1}{\partial \eta} + \xi_y \frac{\partial G_1}{\partial \xi} + \eta_y \frac{\partial G_1}{\partial \eta} \right] \tag{14}$$

where

$$D = \xi_x \eta_y - \xi_y \eta_x$$

$$W = \begin{pmatrix} \rho \\ \rho u \\ \rho v \end{pmatrix}, \quad F = \begin{pmatrix} \rho u \\ \rho u^2 + p \\ \rho uv \end{pmatrix}, \quad G = \begin{pmatrix} \rho v \\ \rho uv \\ \rho v^2 + p \end{pmatrix} \quad F_1 = \begin{pmatrix} 0 \\ \tau_{xx} \\ \tau_{xy} \end{pmatrix} \quad G_1 = \begin{pmatrix} 0 \\ \tau_{xy} \\ \tau_{yy} \end{pmatrix} \tag{15}$$

This formulation is termed the quasi-linear form and has been used successfully for a number of cascade and airfoil calculations (Refs. 13, 32 and 33) for both laminar and turbulent flow in the subsonic regime, however, the formulation has not yet been used in the transonic regime. For transonic flow two additional items must be considered; these are the choice of dependent variables and the use of the "quasi-linear" equation form Eq. (14) rather than the strong conservation form, which is written as

$$\frac{\partial W/D}{\partial \tau} + \frac{\partial}{\partial \xi}\left[\frac{W\xi_t}{D} + \frac{F\xi_x}{D} + \frac{G\xi_y}{D}\right] + \frac{\partial}{\partial \eta}\left[\frac{W\eta_t}{D} + \frac{F\eta_x}{D} + \frac{G\eta_y}{D}\right] - \frac{1}{Re}\left[\frac{\partial}{\partial \xi}\left(\frac{F_1\xi_x}{D} + \frac{G_1\xi_y}{D}\right) + \frac{\partial}{\partial \eta}\left(\frac{F_1\eta_x}{D} + \frac{G_1\eta_y}{D}\right)\right] \qquad (16)$$

Considering the first of these items, when transonic flow is considered, two obvious choices for dependent variable sets arise. These are the primitive set of dependent variables, ρ, u, v and the mass flux set of dependent variables ρ, ρu, ρv. Within the framework of the LBI procedure (Ref. 14) the steady converged solution obtained using either set of dependent variables will be the same; however, differences will occur if an artificial dissipation term is added to the equations. Therefore, for convenience the same primitive set of dependent variables is used here as was used in previous subsonic calculations (Ref. 13). Furthermore, based upon the results of the one-dimensional Rayleigh problem with heat addition, second-order dissipation based upon the variables ρ, u, v is used. The second item to be considered concerns the choice of Eq. (14) or Eq. (16) and results of good quality have been obtained for steady flows using the "quasi-linear" formulation, Eq. (14) for subsonic airfoil and cascade flows (Refs. 13, 31 and 32). Further, since the metric coefficients are independent of the flow being transonic and since

---

32. Shamroth, S. J. and H. J. Gibeling: A Compressible Solution of the Navier-Stokes Equations for Turbulent Flow about an Airfoil. NASA CR-3183, 1979. (Also AIAA Paper 79-1543).

33. Shamroth, S. J. and H. J. Gibeling: Analysis of Turbulent Flow about an Isolated Airfoil with a Time-Dependent Navier-Stokes Procedure. Paper presented at AGARD Specialists Meeting on Boundary Layer Effects on Unsteady Airloads, Aix-en-Provence, France, September 1980.

results obtained via Eq. (14) are less sensitive to the method used to evaluate the metric coefficients than are results obtained via Eq. (16), Eq. (14), the quasi-linear form was used in the present effort.

Boundary Conditions

The final item to be presented prior to performing cascade calculations concerns boundary conditions. The boundary conditions used in the present calculations followed the suggestion of Briley and McDonald (Ref. 34); these were used successfully in the previous cascade study described in Ref. 13. For the cascade system shown in Fig. 10, AB and CD are periodic boundaries and periodic conditions are set here. It should be noted that specification of periodic boundary conditions is simplified considerably if the metric data is continuous at periodic lines. If the metric data is not continuous, devices such as special difference molecules or one-sided differencing is required and in general these devices introduce logical complexity and may cause the solution to suffer a loss of accuracy. The present grid is orthogonal at the periodic line and, therefore, the metric coefficients are continuous across this line. With the present grid construction process, application of the periodic boundary conditions is a straight-forward task.

Specifications of upstream and downstream conditions is somewhat more difficult. For an isolated cascade, boundary conditions for the differential equations may be known at both upstream infinity and downstream infinity. However, since computation economics argues for placing grid points in the vicinity of the cascade and minimizing the number of grid points far from the cascade, the upstream and downstream computational boundaries should be set as close to the cascade as is practical. In addition, with the particular body-fitted coordinates used as the upstream boundary moves further upstream, the angle between pseudo-radial and pseudo-azimuthal coordinate lines becomes smaller. Decreasing the coordinate angle causes the coordinate system to become less well-conditioned and increases the role of cross-derivative terms in the equations. Both of these characteristics could be detrimental to the

---

34. Briley, W. R. and H. McDonald: Computation of Three-Dimensional Horseshoe Vortex Flow Using the Navier-Stokes Equations. 7th International Conference on Numerical Methods in Fluid Dynamics, June 1980.

present numerical procedure and, therefore, they also argue for placing the upstream boundary as close to the cascade as possible. However, when the upstream boundary is placed close to the cascade, most flow function conditions on the boundary will not be known.

In the present approach the suggestion of Ref. 34 is followed which sets total pressure on boundary BC. Unless boundary BC is very far upstream, the flow velocity along this boundary will not be equal to the velocity at upstream infinity since some inviscid deceleration will have occurred. However, as long as the boundary is upstream of the region of any significant viscous or shock phenomena, the total pressure on this boundary will be equal to the total pressure at upstream infinity. Hence, total pressure is an appropriate boundary condition. In addition to specifying upstream total pressure, it is necessary to specify the inlet flow angle. In the present calculation a value was simply assumed. A more accurate specification of the inlet flow angle could be the embedding of a viscous region surrounding the cascade within a large inviscid flow field. Zone embedding processes have been discussed in some detail by McDonald and Briley in Ref. 35. Obviously, the current specification is a simple one. An alternate and quite feasible specification of the inlet flow angle could be based upon an inviscid solution for the cascade and this could be improved by using an interaction between the viscous and inviscid analyses to allow viscous phenomena occurring near the blades to affect the flow angles at the upstream boundary. This refinement is not included at the present stage of development of the analysis. The third condition set on the upstream boundary concerns the density and several possibilities exist. Either the first or second normal derivatives can be set to the inviscid value or be set to zero. In the present application the first derivative of density was set to zero.

The downstream boundary was treated by setting a constant static pressure and by setting second derivatives of both velocity components equal to zero at this location. In the present application the static pressure was set as the pressure at downstream infinity, and hence it is assumed that the downstream

---

35. McDonald, H. and W. R. Briley: Computational Fluid Dynamic Aspects of Internal Flows. AIAA Paper No. 79-1445, 1979.

boundary is located in a region where pressure is uniform. However, as with the inlet flow angle it would be possible to calculate the pressure along this boundary with an inviscid analysis and, if necessary, to interact the viscous and inviscid analyses as the flow progresses.

Both the upstream and downstream boundaries have boundary conditions associated with them which are nonlinear functions of the independent variables. These are the specifications of total pressure on the upstream boundary and static pressure on the downstream boundary. These nonlinear boundary conditions are linearized in the same manner as the governing equations, and then solved implicitly along with the interior point equations.

The final boundary conditions to be considered are the conditions along the blade surface. Here no-slip and no-through flow conditions were applied leading to a specification of zero velocity on the surface. An inviscid transverse momentum equation was applied on the surface leading to a boundary condition approximtion of zero transverse pressure gradient being applied.

IV. RESULTS

As a result of the advances made in the coordinate system generation process it becomes practical to apply the Navier-Stokes calculation procedure to realistic cascade geometries. The geometry chosen is the so-called Jose Sanz controlled diffusion cascade, with solidity, $\sigma = c/H$, equal to approximately 0.94, an inlet flow angle of 35.8° and an exit geometry angle of 0°. For the purpose of the calculation, the trailing edge was brought to a cusp to allow use of a 'C'-type coordinate grid. The solidity ratio is defined as the ratio of chord, c, to distance between periodic lines, H. The flow conditions chosen were Reynolds number based upon chord and downstream conditions of 1.2×10^6, which gives largely turbulent flow over the cascade, and a nominal approach Mach number of 0.75. Since the boundary conditions set total pressure at the upstream boundary and static pressure at the downstream boundary, the Mach number on the upstream boundary is not set a priori but evolves from the solution and is controlled by the ratio of these quantities.

The calculations were carried out on a highly stretched grid having 113 pseudo-azimuthal points and 30 pseudo-radial points; i.e., referring to Fig. 10, 113 pseudo-radial lines such as A A' and 30 pseudo-azimuthal loops A'E'D' were used. Grid points were packed to obtain high resolution both in the vicinity of the blade surface and in the vicinity of the blade leading edge. The first point off the surface was placed at 0.00004 chords from the surface; in contrast the distance between grid points in the center region of the passage reached a value of 0.06 chords. Similarly the distance between grid points on the blade surface in the vicinity of the blade stagnation point was also kept small having a value of .0046 chords at the blade leading edge. In contrast, the grid spacing at the downstream boundary was 0.16 chords, the downstream boundary being taken two chords downstream of the blade trailing edge.

The calculations were initiated by assuming uniform flow with a boundary layer correction on the airfoil surface. The calculation was run first as a variable viscosity laminar flow and after the basic flow pattern began to develop, a mixing length turbulence model was initiated. The calculations were run using a time-scaling technique developed by McDonald and Briley (Ref. 35), and previously used for cascade flows by Shamroth, Gibeling and McDonald (Ref. 13). This technique in conjunction with the existing LBI Navier-Stokes calculation procedure (Ref. 14) leads to a very efficient numerical procedure

which converged rapidly. Convergence was obtained from the initial start in approximately 150 time steps with convergence being determined by monitoring the time history of the flow at selected points in the field as well as the time history of the surface pressure distribution. No attempt was made to optimize convergence so it may be possible to converge the solution in less than 150 time steps. The calculation for this grid required approximately 15 seconds of CDC 7600 time per time step. However, the code used to implement the algorithm is still a research code with a large amount of overhead computation. With some recoding it is believed run time per time step could be reduced substantially.

Three cases were calculated. The first case corresponds closely to the inviscid calculation presented in Ref. 6 with the upstream flow angle being 30.8° and the converged upstream Mach number being 0.72. The case was calculated using second-order artificial dissipation in both coordinate directions to eliminate spatial oscillations. In previous subsonic calculations for both isolated airfoils (Refs. 32 and 33) and cascades (Ref. 13) reasonable results had been obtained with the dissipation parameter equal to 0.5 in both the pseudo-radial and pseudo-azimuthal directions. Although these values appeared reasonable for shock free flow, the one-dimensional study previously described indicates a lower value should be used in the direction normal to the shock. Therefore, in this first case the pseudo-azimuthal dissipation parameter was taken to be .05 with an intention of investigating lower values (σ = .025) subsequently. Since the model Rayleigh problem focuses upon the shock capturing aspects of the transonic cascade analysis, it does not give guidance as to a choice for the dissipation parameter in the pseudo-radial direction where normal diffusion rather than axial diffusion is a major contributor to the momentum balance. Therefore, the diffusion parameter in this direction was kept at the previously used value of 0.5. It should be noted that with the small pseudo-radial grid spacing in the vicinity of the blade boundary ($\Delta n/c = 4 \times 10^{-5}$) and with the small transverse velocities in this region ($v/u < .05$) little pseudo-radial artificial dissipation was added in the boundary layer region; the major effect of pseudo-radial artificial dissipation is in the cascade center region. Although this appears reasonable particularly since the shock is nearly parallel to the pseudo-radial direction, the role of this artificial dissipation mechanism must still be investigated further. Such a study is envisaged in the near future.

During the calculation of the $\sigma = .05$ cases, it became apparent that although the pseudo-azimuthal dissipation parameter of 0.05 was adequate in the vicinity of the shock, it was not adequate in the leading edge region. This region contained very large spatial oscillations when the run was made under the $\sigma = .05$ conditions. Therefore, σ was made a function of distance from the leading edge being taken as 0.5 at the leading edge and decreasing smoothly to a value of 0.05 by the ten per cent chord station. It is anticipated that the necessity to increase σ in the leading edge is related to a lack of spatial resolution and with better spatial resolution the pseudo-azimuthal dissipation parameter could be set to 0.05 throughout the flow.

Although some differences between viscous and inviscid solutions should exist, they should be consistent with the inclusion of viscous phenomena. A comparison between the inviscid calculation and the current viscous calculation with $Re \approx 1.2 \times 10^6$ and $M = 0.72$ is presented in Fig. 11. As can be seen in Fig. 11, the results of the two procedures compare quite well in the leading edge region. The maximum suction peak value in the viscous solution is slightly higher than that obtained in the inviscid solution; however, both peaks occur at the same location. Differences in the trailing edge surface pressure distributions are consistent with the inclusion of boundary layer development in the viscous solution. Although a full quantitative assessment must await an extensive data comparison program, the results shown in Fig. 11 demonstrate the Navier-Stokes results to be consistent with inviscid results at high chord Reynolds numbers and low incidence, as expected.

The second and third cases considered serve to show details of the flow field and the effect of the dissipation parameter, σ. In Case II, the dissipation parameter was taken to be 0.5 in both the pseudo-radial and pseudo-azimuthal directions. The ratio of upstream total pressure to downstream static pressure was taken as 1.48 and the upstream Mach number of the converged solution was approximately 0.78. The third case considered is similar to Case II with the dissipation parameter in the pseudo-radial direction being taken as 0.05. Rather than keep the ratio of upstream total to downstream static pressure consistent with that of Case II, the downstream static pressure was varied so as to match the inlet Mach number of 0.78 at the upstream boundary in both cases. In other words the cases were run at the same upstream total conditions with the downstream pressure being varied to obtain the same upstream Mach number. A Mach number of 0.78 was obtained in this case when the ratio of upstream

total pressure to downstream static pressure was 1.40. This is consistent with a lower loss level at the lower value of the dissipation parameter.

Prediction of the surface pressure distribution for the two values of dissipation parameter is shown in Fig. 12 where the effect of artificial dissipation is evident. Although the surface pressure distribution remained smooth when the dissipation parameter was 0.05, spatial oscillations occurred in the density field away from the wall in the vicinity of the shock and had an amplitude of approximately four per cent of the mean density value. These oscillations were not present in the model problem even when the dissipation parameter was reduced to .025 and their appearance here is indicative of the more complex flow field present in the cascade. Since some oscillations appeared when the dissipation parameter was taken as .05, no attempt was made to reduce this value to .025 as it was felt that this would increase the amplitude of the oscillation. As can be seen in the figure, setting the dissipation parameter to 0.5 for the pseudo-azimuthal (streamwise) direction gives considerable non-physical smoothing in the region of the shock and reduces the suction peak from a value of -1.5 at a dissipation parameter of .05 to a value of -1.16 at a dissipation parameter of .5. Obviously, the use of the dissipation parameter equal to .5 for the azimuthal direction has had a very adverse effect upon accuracy for this calculation. On the other hand the 0.05 dissipation parameter gives a sharp representation of the pressure rise. The streamwise grid spacing in the vicinity of the shock is $\Delta x/c \approx .03$ and although the pressure rise is smeared in the wall region due to the shock boundary layer interaction, it is very sharp in regions removed from the boundary layer. For example, at a distance of 0.05c above the suction surface the pressure coefficient rises from -1.44 to -0.31 in four grid points.

Contours of Mach number for the two cases are presented in Figs. 13 and 14. The outer boundaries are periodic lines and the plotting routine draws the coordinate system branch cut emanating from the airfoil trailing edge. For the .5 dissipation parameter calculation, Fig. 13, the maximum Mach number reached is approximately 1.17 and the Mach number decrease as the flow proceeds over the suction surface is very gradual. In contrast the maximum Mach number for the .05 dissipation parameter calculation is 1.56 and a rapid deceleration resembling a shock wave occurs downstream of this maximum. A comparison of Mach number contours for the flow field above the suction surface shows the strong effect of dissipation parameter and indicates setting the dissipation

parameter to .5 is inappropriate with this mesh distribution and density for flows having shock waves. As previously discussed, the azimuthal σ = .05 calculation showed some slight spatial oscillations in density ($\approx 4\%$) which may require further attention, however, as seen in the figures, realistic solutions were obtained. It should be noted that the effect of artificial dissipation was considerably less on the pressure surface flow field and in the blade wake region where no shock occurred. Velocity contours which give the magnitude of the velocity vector are presented in Figs. 15 and 16. The results here are consistent with the Mach number results.

Velocity vector plots for both cases are given in Figs. 17 and 18. For clarity, only the velocity vectors at selected points are plotted. The velocity direction is specified on the inflow boundary, however, the flow angle is not specified on the outflow boundary and the observed flow turning results from the calculation. The predicted flow angle at the outflow boundary (which is two chords downstream of the trailing edge and not shown on this figure) is approximately 6 degrees in both cases. The predicted turning of the flow as it passes through the cascade is evident as is the rapid deceleration on the suction surface. As shown in Figs. 17 and 18, both calculations predict separation to occur on the suction surface. Although separation is possible, particularly in the presence of a shock, this result requires experimental confirmation. It is possible that the prediction of separation may be influenced by the simple turbulence model used and a comparison with data may indicate the need for further work in this area. The vertical arrows occurring at the airfoil surface are data points having zero velocity (no-slip conditions).

Contours of static pressure coefficient are presented in Figs. 19 and 20. Although not shown on this plot, the stagnation point pressure coefficients for the both σ = .5 and σ = .05 cases were 1.07. This is somewhat lower than the value of 1.16 which would be expected from inviscid considerations and the discrepancy may be due to viscous effects, numerical truncation or a failure to resolve the Heimenz layer. The differences in pressure coefficient between the two cases are again more evident over the suction surface. The ratio of outflow to inflow static pressure for the cases is 1.03 and 1.1 respectively. A one-dimensional inviscid estimate of the pressure ratio gives $p_{out}/p_{in} \approx 1.28$ and, therefore, the predicted pressure rise is less than the inviscid estimate. This difference represents losses, with the greater losses occurring in the σ = .5

case, the case having larger artificial dissipation. Predictions of total pressure coefficient, $(p_t - p_\infty)/(1/2\ \rho_\infty u_\infty^2)$, are given in Figs. 21 and 22, respectively. These low total pressure regions are confined to the boundary layer and the wake.

V. CONCLUDING REMARKS

In the present study, several questions relevant to the viscous transonic cascade problem have been posed and answered by considering simple flow situations. These questions focused upon spatial differencing, specification of boundary conditions and use of artificial dissipation in flows containing shock waves. In regard to the first of these problems, the model problem clearly shows that converged solutions can be obtained using spatial central difference representations in both subsonic and supersonic portions of the flow. A study of boundary conditions in a simple one-dimensional problem indicated that for flows having subsonic inflow and outflow conditions, specification of total pressure on the upstream boundary and static pressure on the downstream boundary is satisfactory and physically realistic. Finally, various methods of calculating flows with shock waves were considered by solving a one-dimensional flow problem with heat sources. Among the methods considered for obtaining stable solutions in the presence of shocks were second-order dissipation methods, fourth-order dissipation methods and pressure damping methods. The results obtained in this model problem indicate that with the envisaged grids, second-order dissipation with a relatively low dissipation parameter, $\sigma \approx .025$, is a suitable method for use in transonic flow problems. Further, it was found preferable to add dissipation terms containing derivatives of the primitive variables ρ, u, w.

Based upon these preliminary studies, a calculation was made of flow through a cascade of Jose Sanz airfoils. In this calculation spatial central differences were used throughout to represent spatial derivatives; boundary conditions consisted of upstream total pressure, total temperature and flow angle and downstream static pressure and second-order artificial dissipation was used to suppress spatial oscillations. The coordinate system used was a constructive 'C'-type system containing 113 pseudo-azimuthal points and 30 pseudo-radial points. The grid contained high resolution in the vicinity of the blade surface and the blade leading edge region. A calculation made for this cascade at low loading predicted a surface pressure distribution in good agreement with inviscid results; the differences were consistent with the inclusion of viscous effects. Two additional calculations were run at higher loading, each having a Reynolds number based upon chord of 1.2×10^6 and a Mach number at the upstream boundary of 0.8. In these calculations, the dis-

sipation parameter in the pseudo-radial direction was set to 0.5. In the first calculation the dissipation parameter in the pseudo-azimuthal direction was taken to be 0.5, however, in the second calculation this value was taken as 0.05. In both cases an embedded supersonic flow region appeared over the suction surface. In the case with dissipation parameter equal to .05 the supersonic region was terminated by a rapid pressure increase representing a shock wave. However, in the 0.5 dissipation parameter case considerable smearing of the results occurred. These results are consistent with the results obtained for the model one-dimensional problem.

The results obtained in the 0.05 dissipation parameter case show the expected qualitative features of transonic cascade flow fields. The flow acceleration around the leading edge suction suface, the flow turning, the development of suction and pressure surface boundary layers and the appearance of an embedded shock are all plainly shown in the figures. Of particular encouragement is the attainment of results for this complex flow field using a dissipation parameter criterion of .05 in the azimuthal direction. The results also show that setting the parameter to 0.5 leads to considerable shock smearing.

When a calculation was initiated as uniform flow with a boundary layer correction, convergence was obtained within 150 time steps; no specific attempt has been made to optimize convergence and, therefore, it is likely that with improved time step selection the number of time steps to reach convergence could be less than this value. The calculations presented clearly demonstrate the practicality of efficiently predicting high Reynolds number transonic cascade flow fields. A constructive coordinate system has been modified to allow specification of realistic cascades and calculations have converged relatively quickly. Although further efforts are called for, particularly in the area of quantitative assessment of results, turbulence modelling and further investigation of artificial dissipation, the results obtained to date are very encouraging.

VI. REFERENCES

1. Delaney, R. A. and P. Kavanagh: Transonic Flow Analysis in Axial-Flow Turbomachinery Cascades by a Time-Dependent Method of Characteristics. ASME Paper No. 75-GT-8, 1975.

2. Gopalakrishna, S. and R. Bozzola: A Numerical Technique for the Calculation of Transonic Flows in Turbomachinery Cascades. ASME Paper No. 71-GT42, 1971.

3. Ives, D. C. and J. F. Liutermoza: Analysis of Transonic Cascade Flows Using Conformal Mapping and Relaxation Techniques. AIAA Journal, Vol. 15, 1977, pp. 647-652.

4. Caspar, J. R., D. E. Hobbs and R. L. Davis: The Calculation of Two-Dimensional Compressible Potential Flow in Cascades Using Finite Area Techniques. AIAA Paper 79-0077, 1977.

5. Erdos, J. I., E. Alzner and W. McNally: Numerical Solution of Periodic Transonic Flow Through a Fan Stage. AIAA Paper 76-369, 1976.

6. Steger, J. L., T. H. Pulliam and R. V. Chima: An Implicit Finite Difference Code for Inviscid and Viscous Cascade Flow. AIAA Paper 80-1427, 1980.

7. McDonald, H.: Computation of Turbomachinery Boundary Layers. The Aerothermodynamics of Aircraft Gas Turbine Engines. AFAPL-TR-78-52, 1978.

8. Levy, R., S. J. Shamroth, H. J. Gibeling and H. McDonald: A Study of the Turbulent Shock Wave Boundary Layer Interaction. Air Force Flight Dynamics Laboratory Report AFFDL-TR-76-163, 1976.

9. Klineberg, J. M. and L. Lees: Theory of Viscous-Inviscid Interactions in Supersonic Flow. AIAA Journal, Vol. 7, 1969.

10. Erdos, J., P. Baronti and S. Elszweig: Transonic Viscous Flow Around Lifting Two-Dimensional Airfoils. AIAA 5th Fluid and Plasma Dynamics Conference, AIAA No. 72-678, 1972.

11. Rehyner, T. and I. Flugge-Lotz: The Interaction of Shock Waves with a Laminar Boundary Layer. International Journal of Nonlinear Mechanics, Vol. 3, 1968.

12. Briley, W. R. and H. McDonald: Numerical Prediction of Incompressible Separation Bubbles. Journal of Fluid Mechanics, Vol. 69, 1975, pp. 631-635.

13. Shamroth, S. J., H. J. Gibeling and H. McDonald: A Navier-Stokes Solution for Laminar and Turbulent Flow Through a Cascade of Airfoils. AIAA Paper No. 80-1426, 1980.

14. Briley, W. R. and H. McDonald: Solution of the Multidimensional Compressible Navier-Stokes Equations by a Generalized Implicit Method. J. Comp. Physics, Vol. 24, No. 4, August 1977, p. 372.

15. Magnus, R. and H. Yoshihara: Inviscid Transonic Flow Over Airfoils. AIAA Journal, Vol. 8, No. 12, pp. 2157-2162, 1970.

16. Murman, E.: Analysis of Embedded Shock Waves Calculated by Relaxation Methods. AIAA Journal, Vol. 12, 1974, p. 626.

17. Jameson, A.: Iterative Solution of Transonic Flows over Airfoils and Sings, Including Flows at Mach 1. Communications on Pure and Applied Mathematics, Vol. 27, 1974, p. 283.

18. Ballhaus, W. F., A. Jameson and J. Albert: Implicit Approximate Factorization Schemes for Steady Transonic Flow Problems. AIAA Journal, Vol. 16, June 1978, pp. 573-597.

19. Jameson, A.: Acceleration of Transonic Potential Flow Calculations on Arbitrary Meshes. AIAA Paper 79-1458.

20. McDonald, H. and W. R. Briley: Computational Fluid Dynamic Aspects of Internal Flows. AIAA Paper 79-1445.

21. Shapiro, A.: The Dynamics and Thermodynamics of Compressible Fluid Flow. Rowland Press, New York, 1958.

22. Roache, P. J.: Computational Fluid Dynamics. Hermosa Press, Albequerque, 1972.

23. Beam, R. M. and R. F. Warming: An Implicit Factored Scheme for the Compressible Navier-Stokes Eqs. Proceedings of AIAA Third Computational Fluid Mechanics Conference, 1977.

24. MacCormack, R. W. and B. S. Baldwin: A Numerical Method for Solving the Navier-Stokes Equations with Application to Shock Boundary Layer Interactions. AIAA Paper 75-1, 1975.

25. Thompson, J. F., F. C. Thames and C. W. Mastin: Boundary Fitted Curvilinear Coordinate Systems for Solution of Partial Differential Equations on Fields Containing Any Number of Arbitrary Two-Dimensional Bodies. NASA Cr-2729, July 1977.

26. Steger, J. L. and R. L. Sorenson: Automatic Mesh Point Clustering Near a Boundary in Grid Generation with Elliptic Partial Differential Equations. Journal of Computational Physics, Vol. 33, 1979, p. 405.

27. Gibeling, H. J., S. J. Shamroth and P. R. Eiseman: Analysis of Strong-Interaction Dynamic Stall for Laminar Flow on Airfoils. NASA CR-2969, April 1978.

28. Eiseman, P. R.: A Coordinate System for a Viscous Transonic Cascade Analysis. United Technologies Research Center Report R76-912149-4, 1976.

29. Eiseman, P. R.: A Coordinate System for a Viscous Transonic Cascade Analysis. J. Comp. Physics, Vol. 26, March 1978, pp. 307-338.

30. Shamroth, S. J. and R. Levy: Description of a Constructive Coordinate System Generation Computer Code for Airfoils. SRA Rpt. R80-1, 1980.

31. Kim, Y.N. and S. J. Shamroth: Revised Coordinate Generation Program for a Cascade of Arbitrarily Shaped Airfoils. SRA Rpt. 81-1, 1981.

32. Shamroth, S. J. and H. J. Gibeling: A Compressible Solution of the Navier-Stokes Equations for Turbulent Flow about an Airfoil. NASA CR-3183, 1979. (Also AIAA Paper 79-1543).

33. Shamroth, S. J. and H. J. Gibeling: Analysis of Turbulent Flow about an Isolated Airfoil Using a Time-Dependent Navier-Stokes Procedure. Paper presented at AGARD Specialists Meeting on Boundary Layer Effects on Unsteady Airloads, Aix-en-Provence, France, September 1980.

34. Briley, W. R. and H. McDonald: Computation of Three-Dimensional Horseshoe Vortex Flow Using the Navier-Stokes Equations. 7th International Conference on Numerical Methods in Fluid Dynamics, June 1980.

35. McDonald, H. and W. R. Briley: Computational Fluid Dynamic Aspects of Internal Flows. AIAA Paper No. 79-1445, 1979.

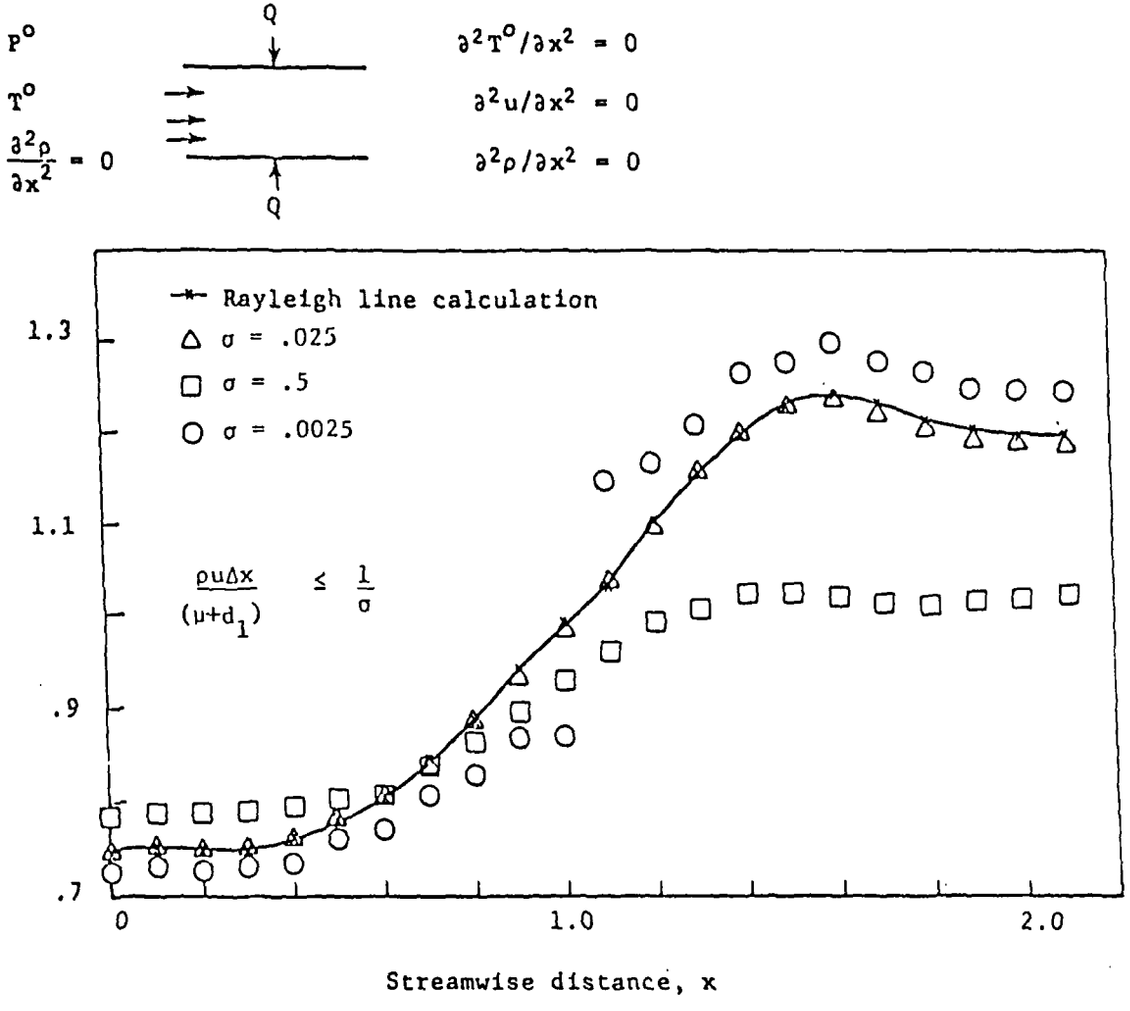

Fig. 1 - Dissipation parameter number study, Case No. 1, supersonic exit flow.

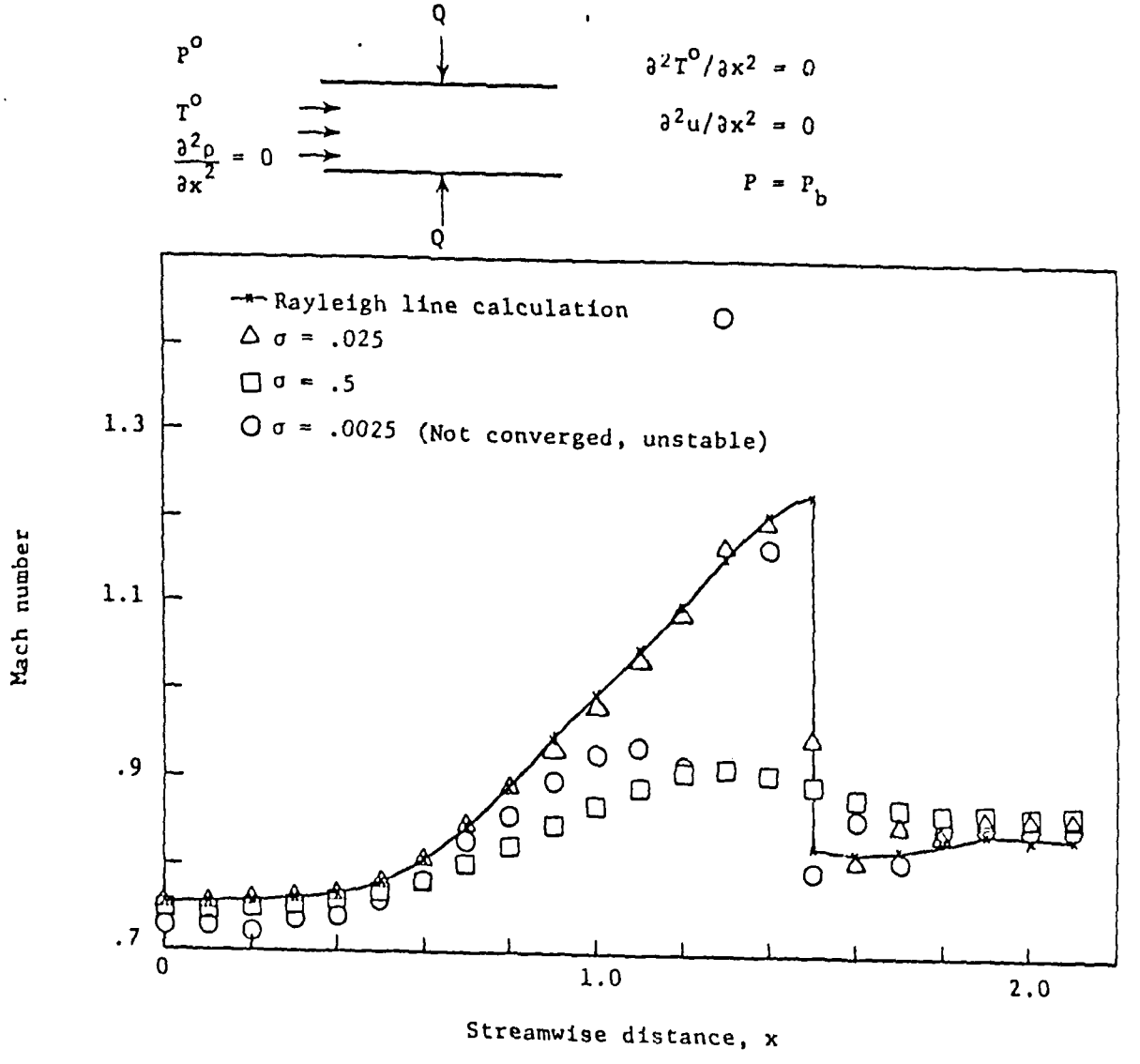

Fig. 2 - Dissipation parameter study, Case No. 2, $P_b = 1.19\ p^*$.

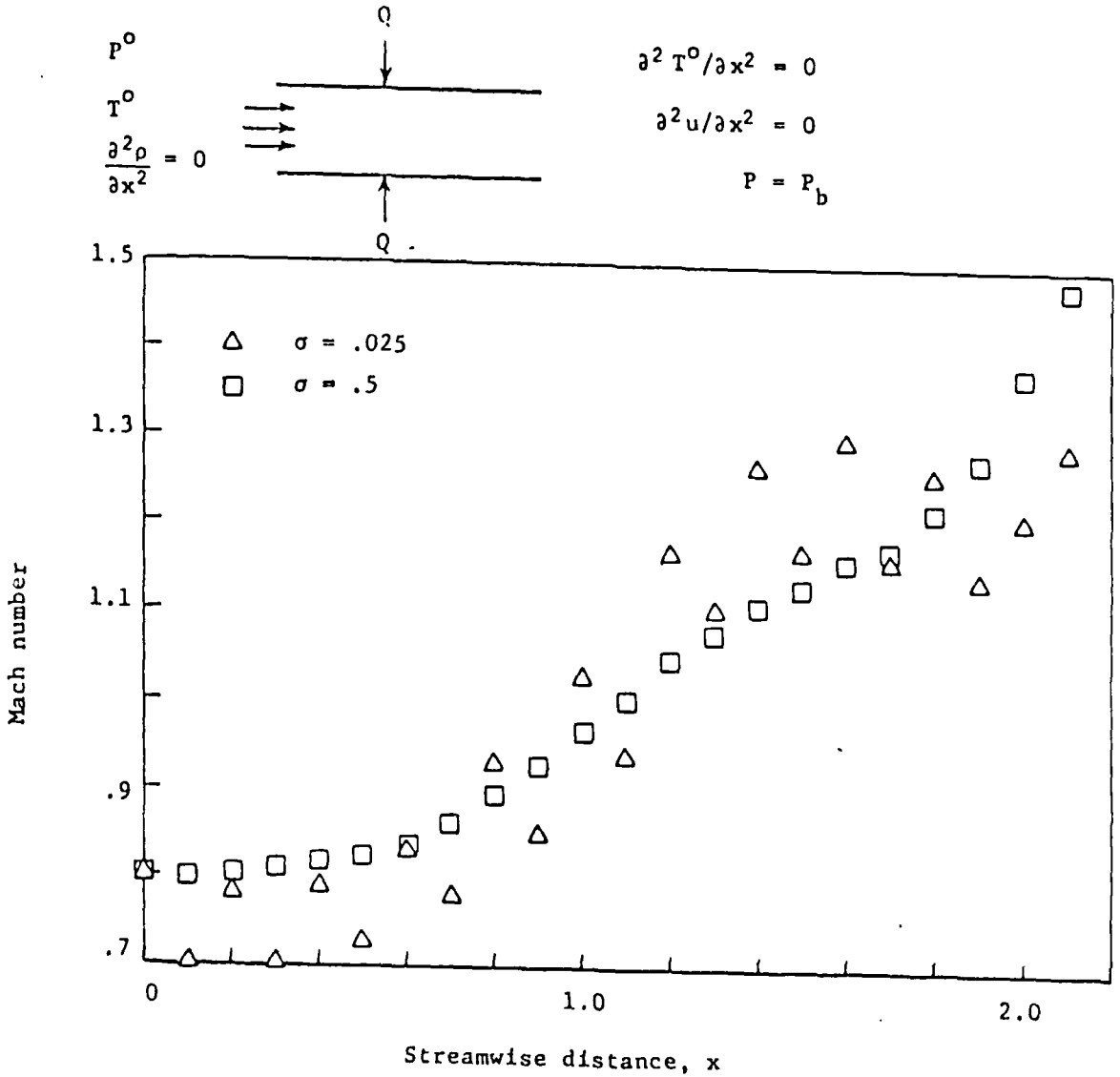

Fig. 3 - Dissipation parameter study, Case No. 3, $P_b = .812\ P^*$.

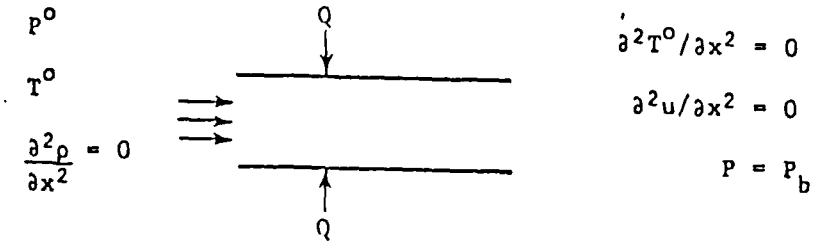

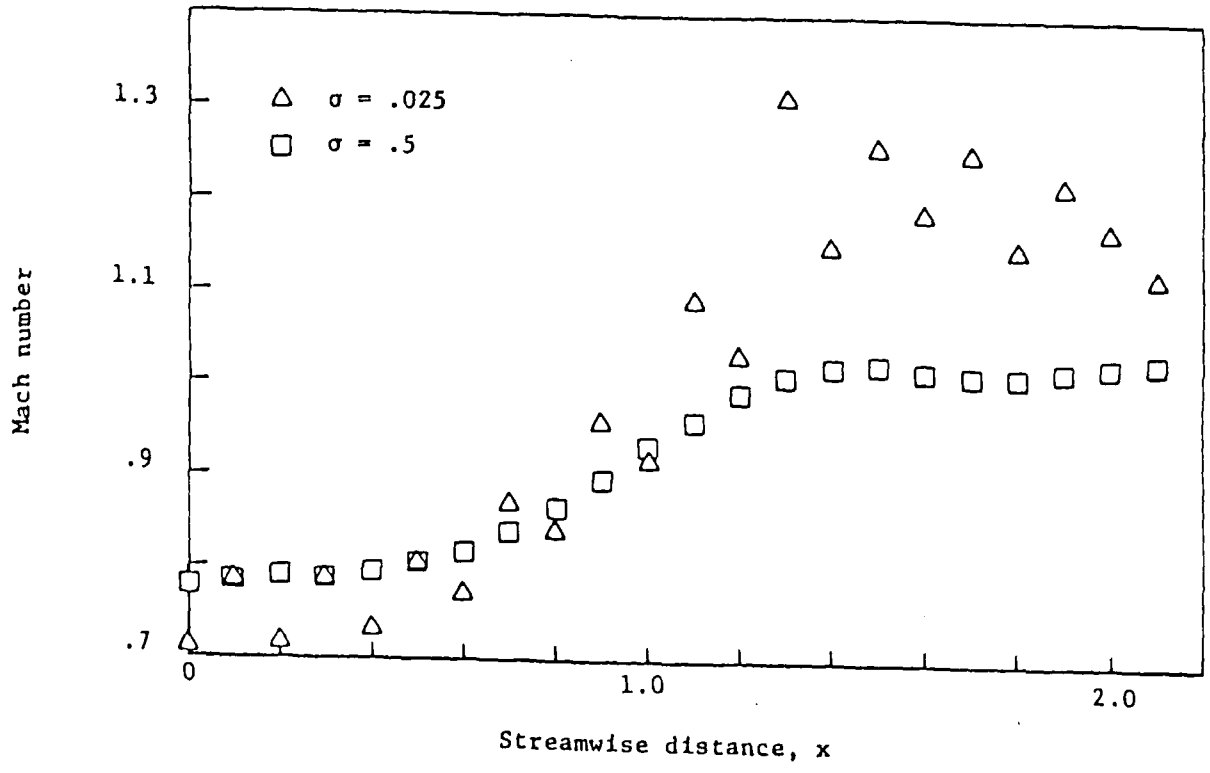

Fig. 4 - Dissipation parameter study, Case No. 4, $P_b = P^*$.

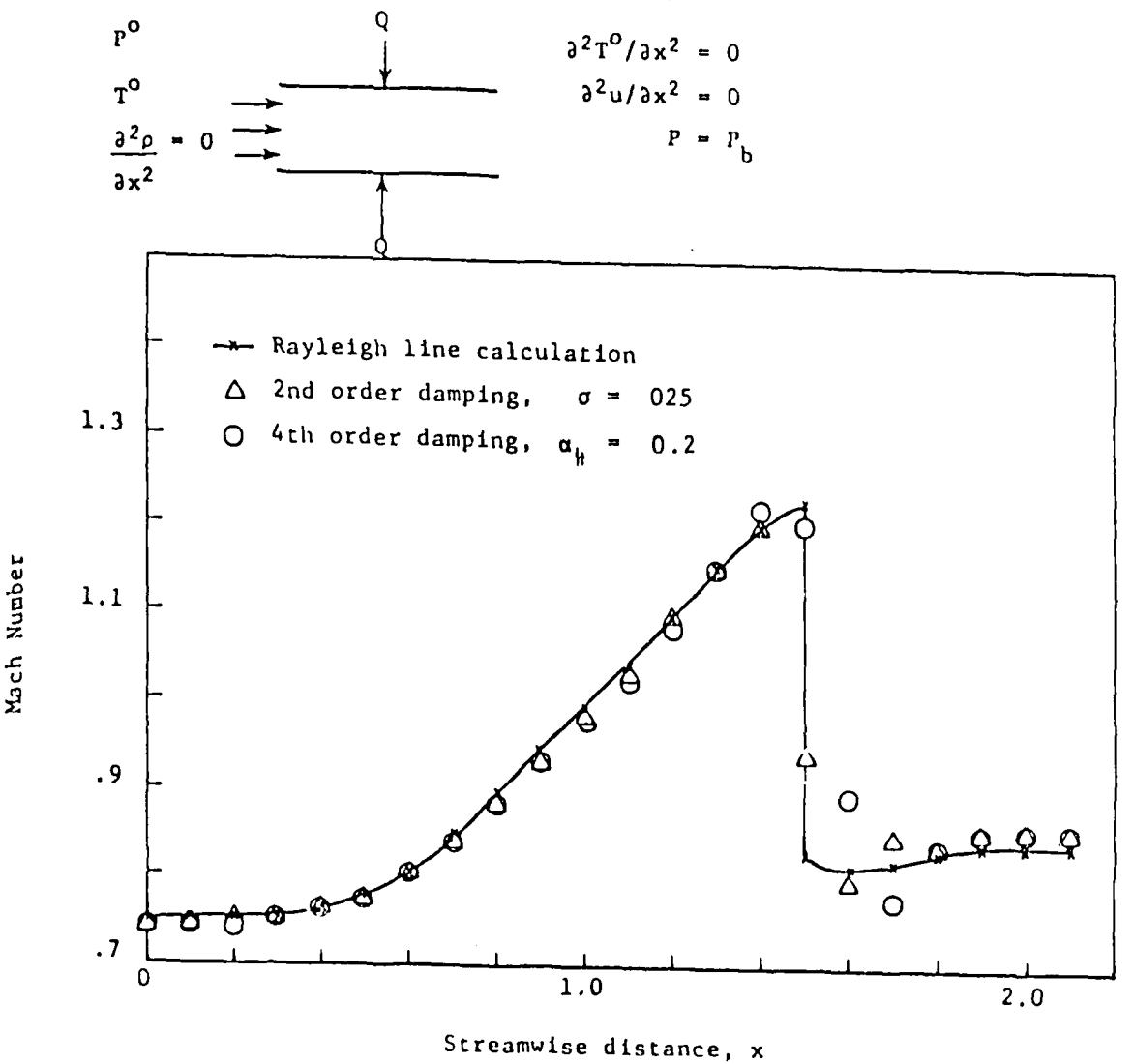

Fig. 5 - Fourth order damping calculation, $P_b = 1.19\ P^*$.

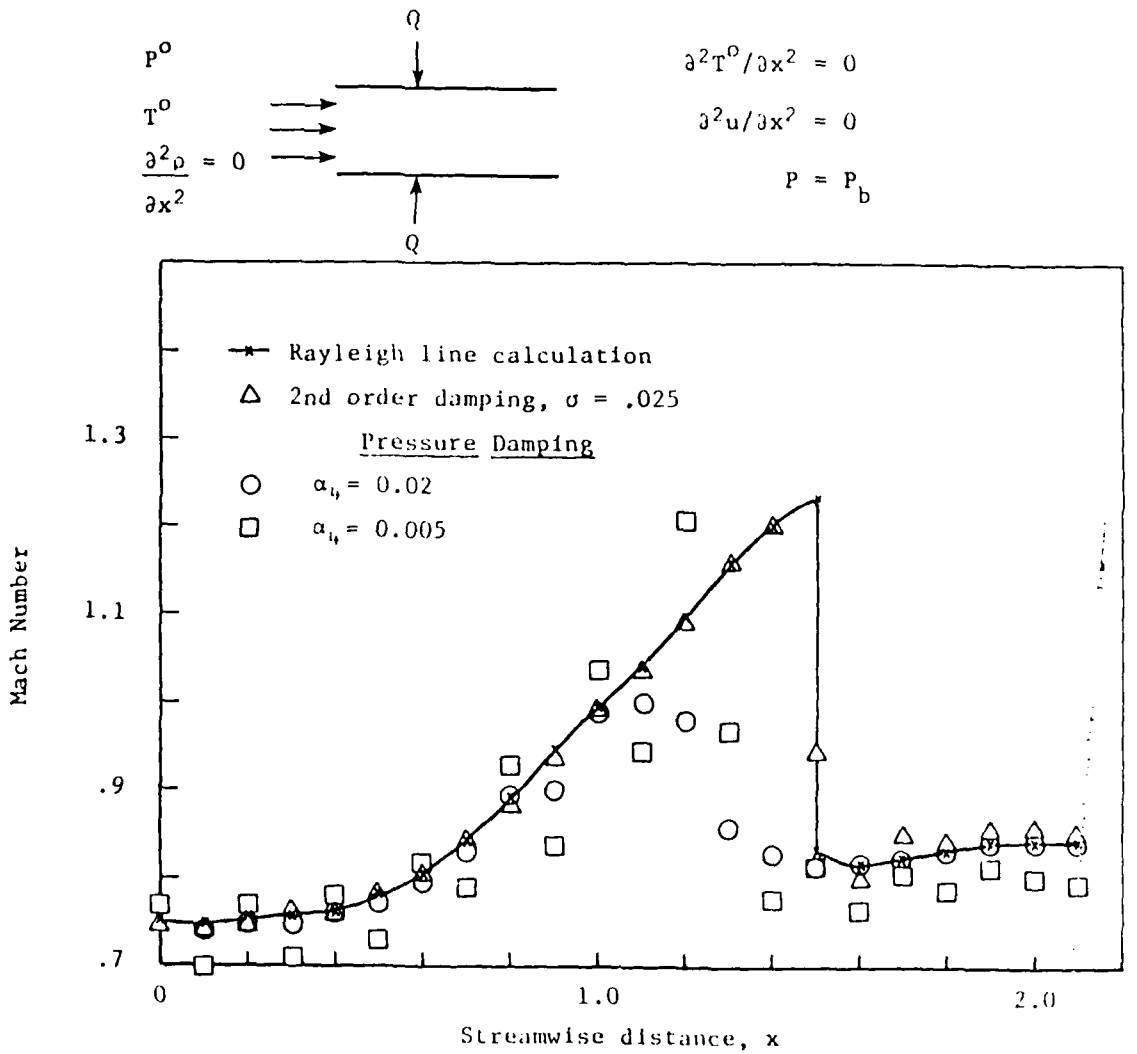

Fig. 6 - Pressure damping calculation, $P_b = 1.19\ p^*$.

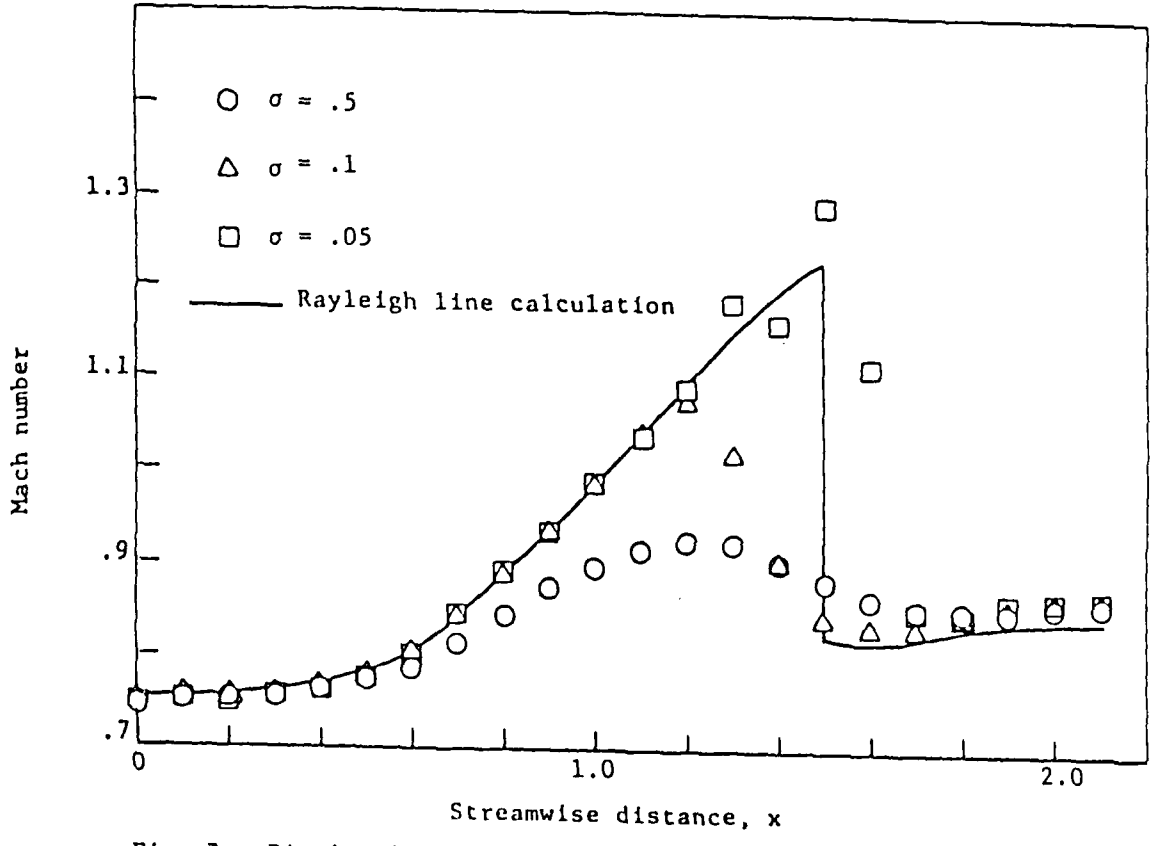

Fig. 7 - Dissipation parameter study; dependent variables, ρ, ρu, T^o; $p_b = 1.19\ p^*$.

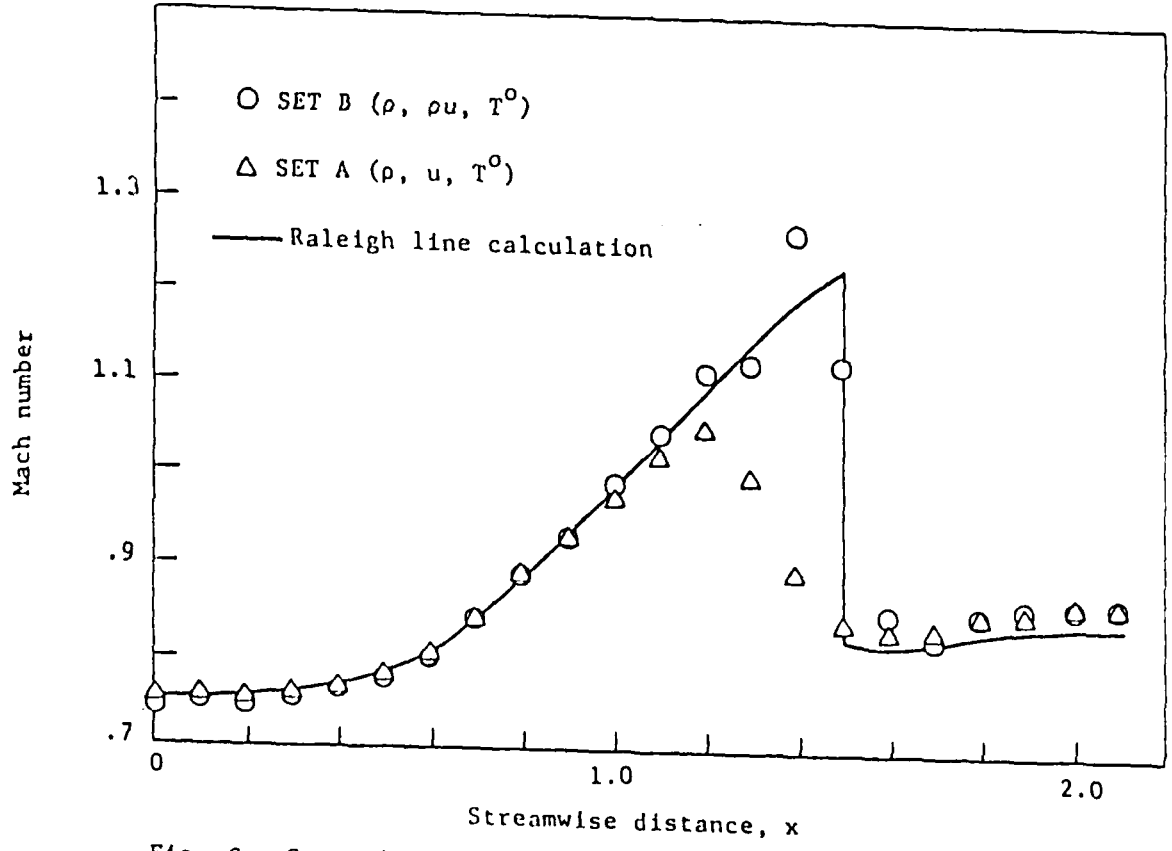

Fig. 8 - Comparison of solutions damping upon different dependent variables, $\sigma = .05$, $p_b = 1.19\ p^*$.

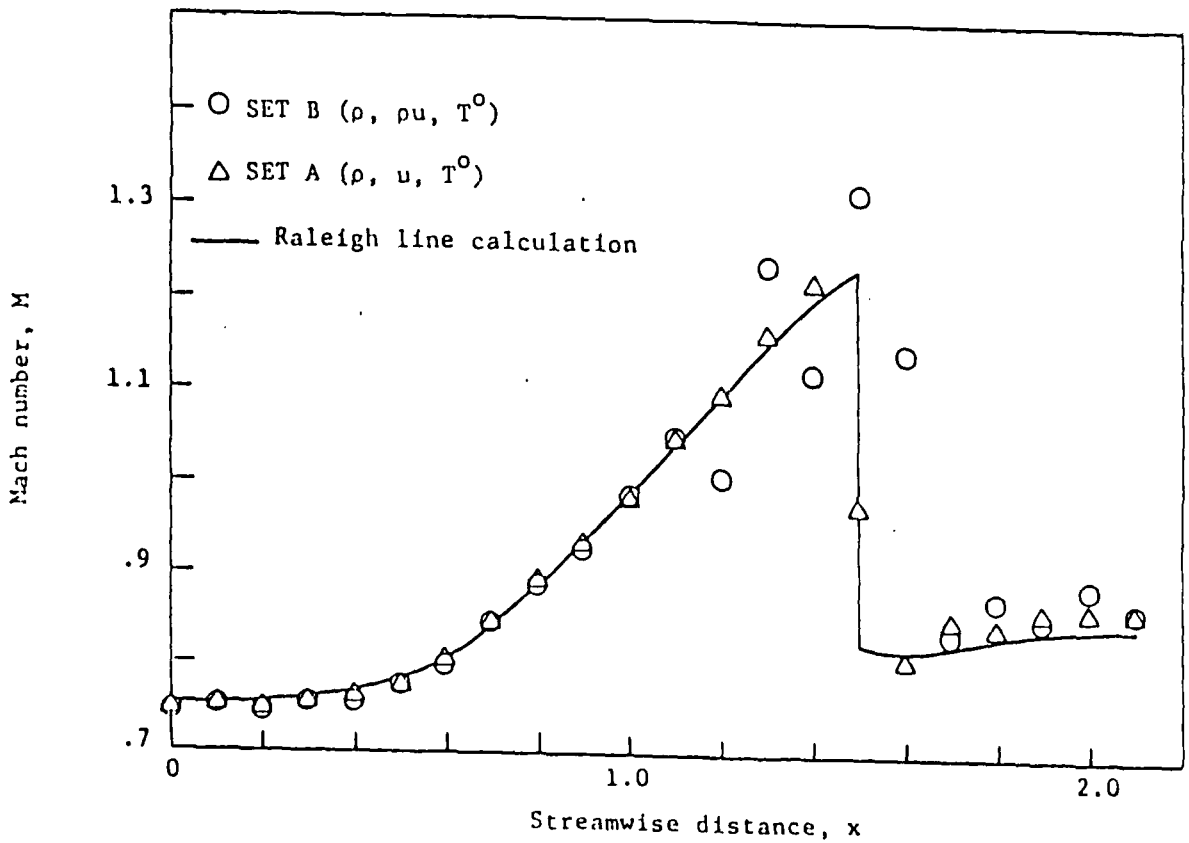

Fig. 9 - Comparison of solutions damping upon different dependent variables, $\sigma = .025$, $p_b = 1.19\ p^*$.

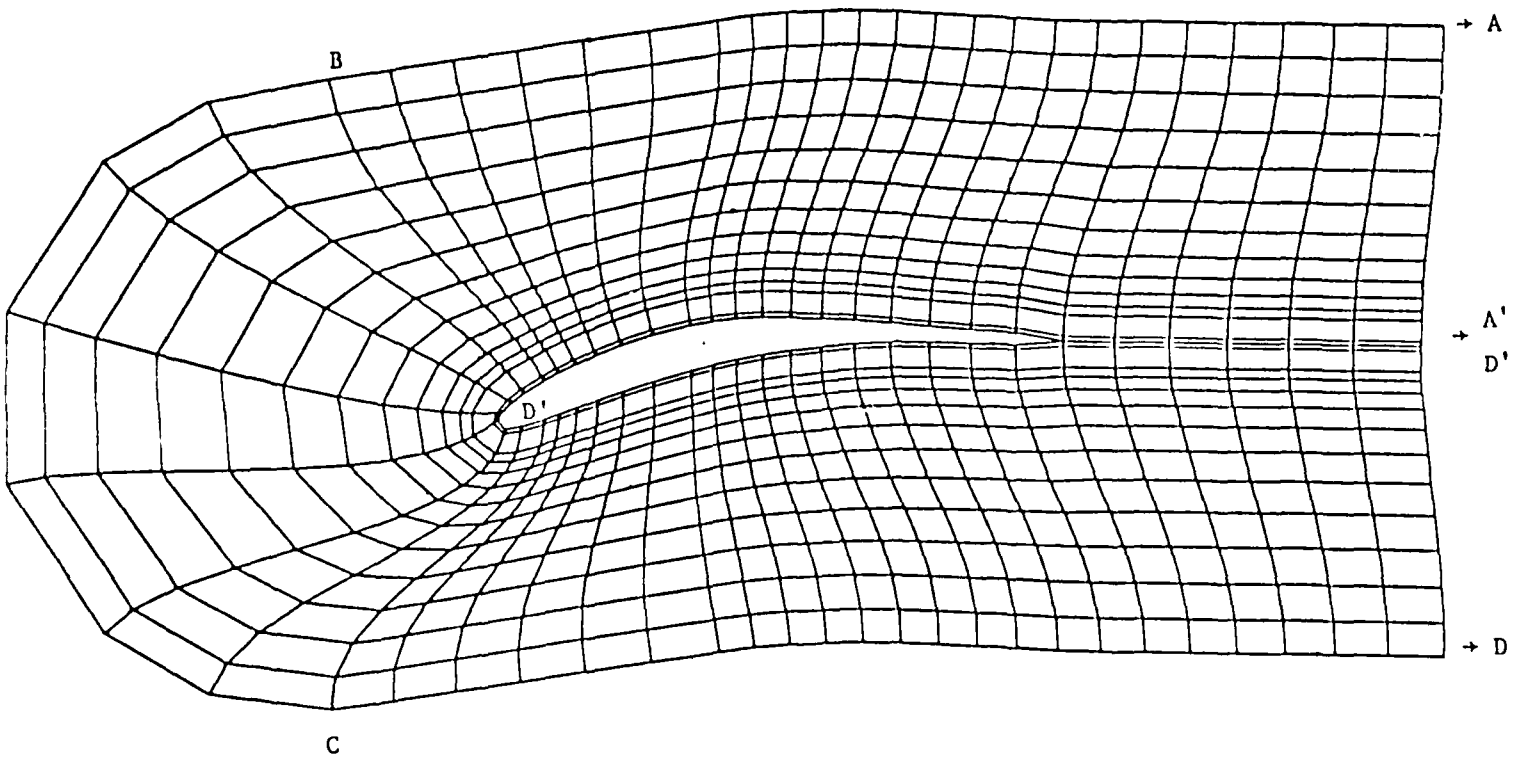

Fig. 10 - Cascade coordinate grid - all grid points not included.

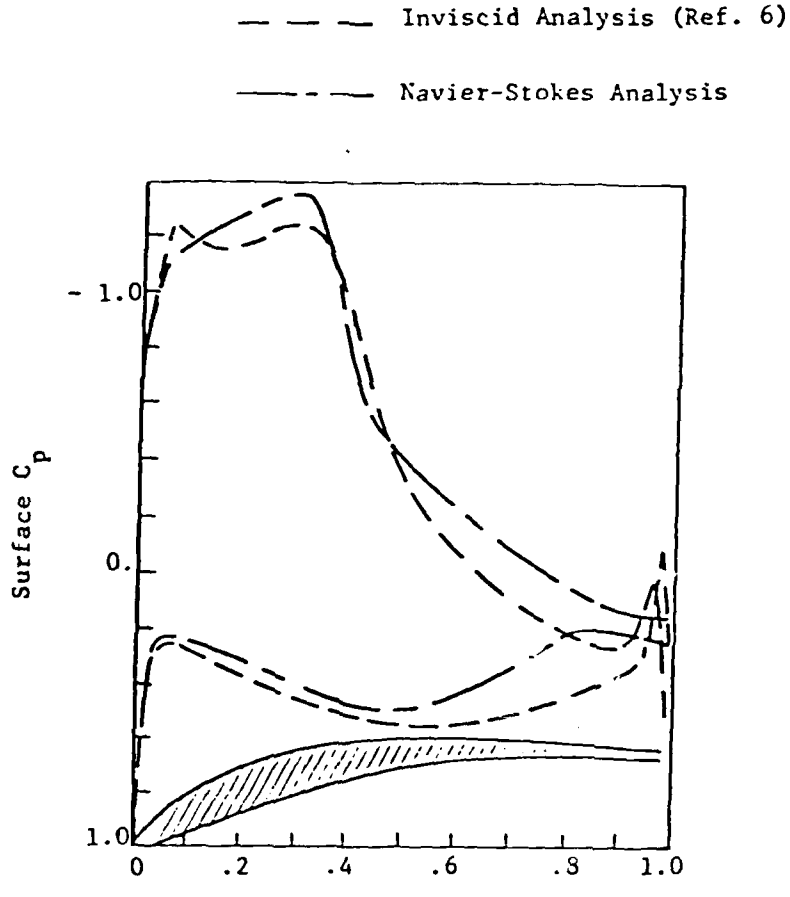

Fig. 11 - Surface pressure distribution.

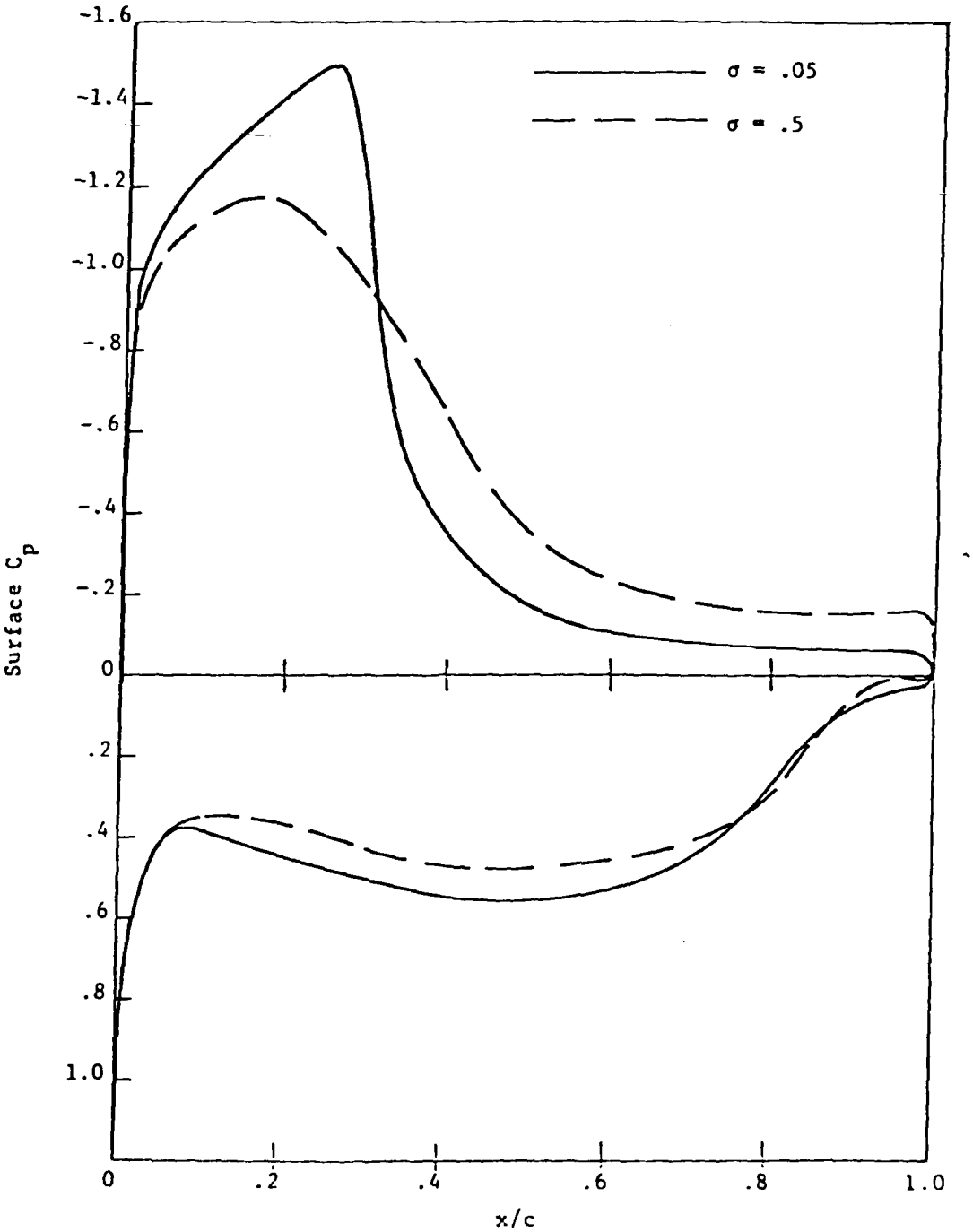

Fig. 12 - Surface static pressure coefficient

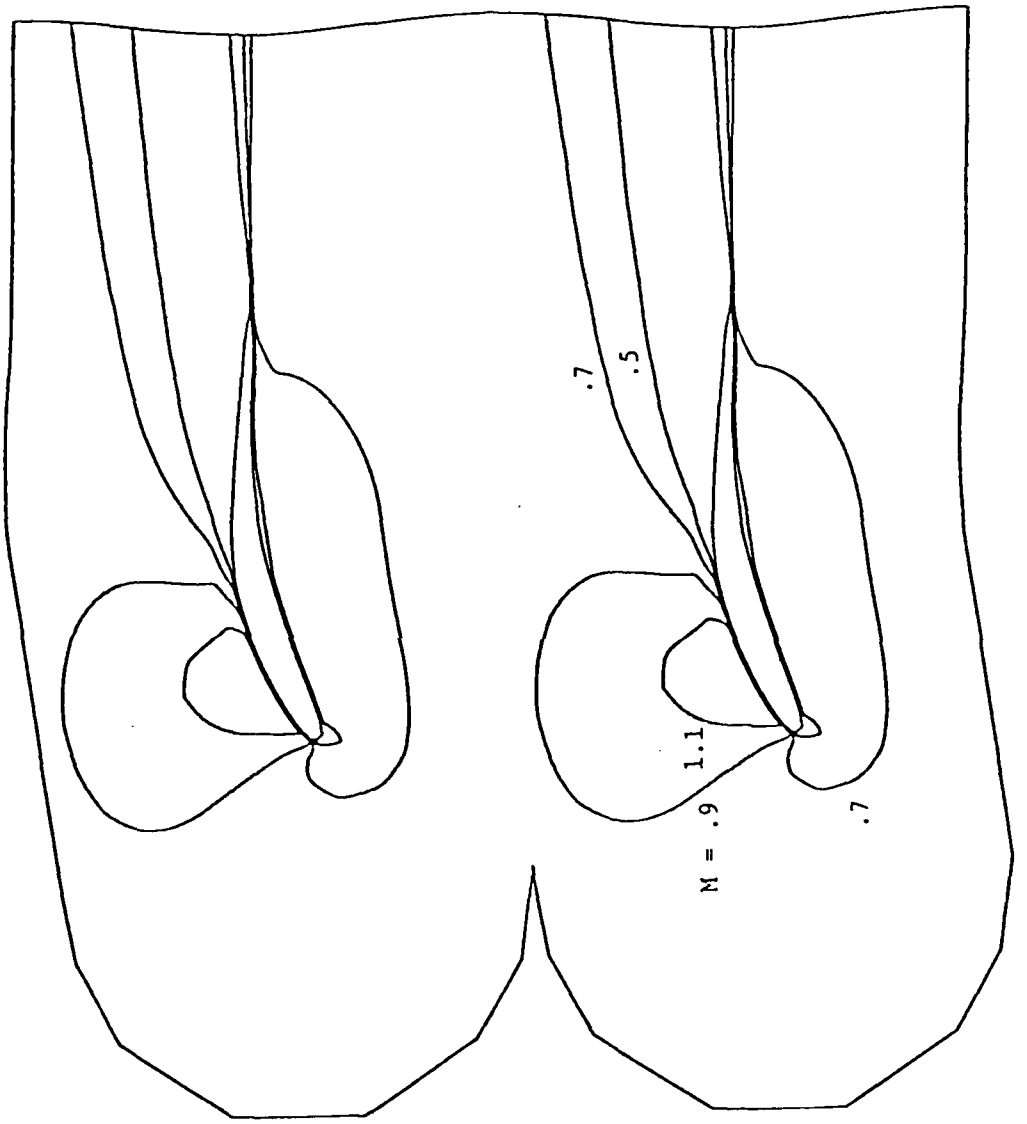

Fig. 13 - Mach number contours, σ = .5.

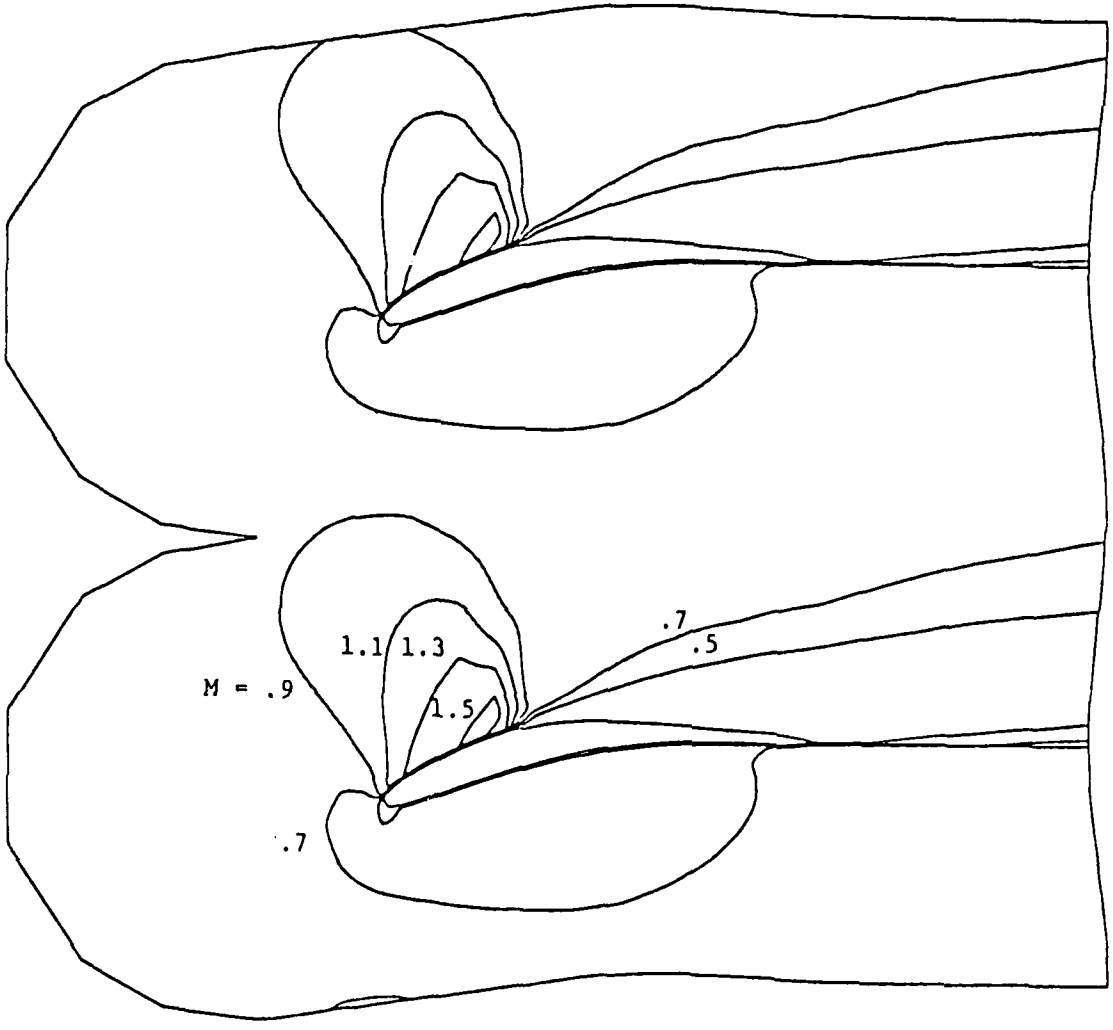

Fig. 14 - Mach number contours, $\sigma = .05$.

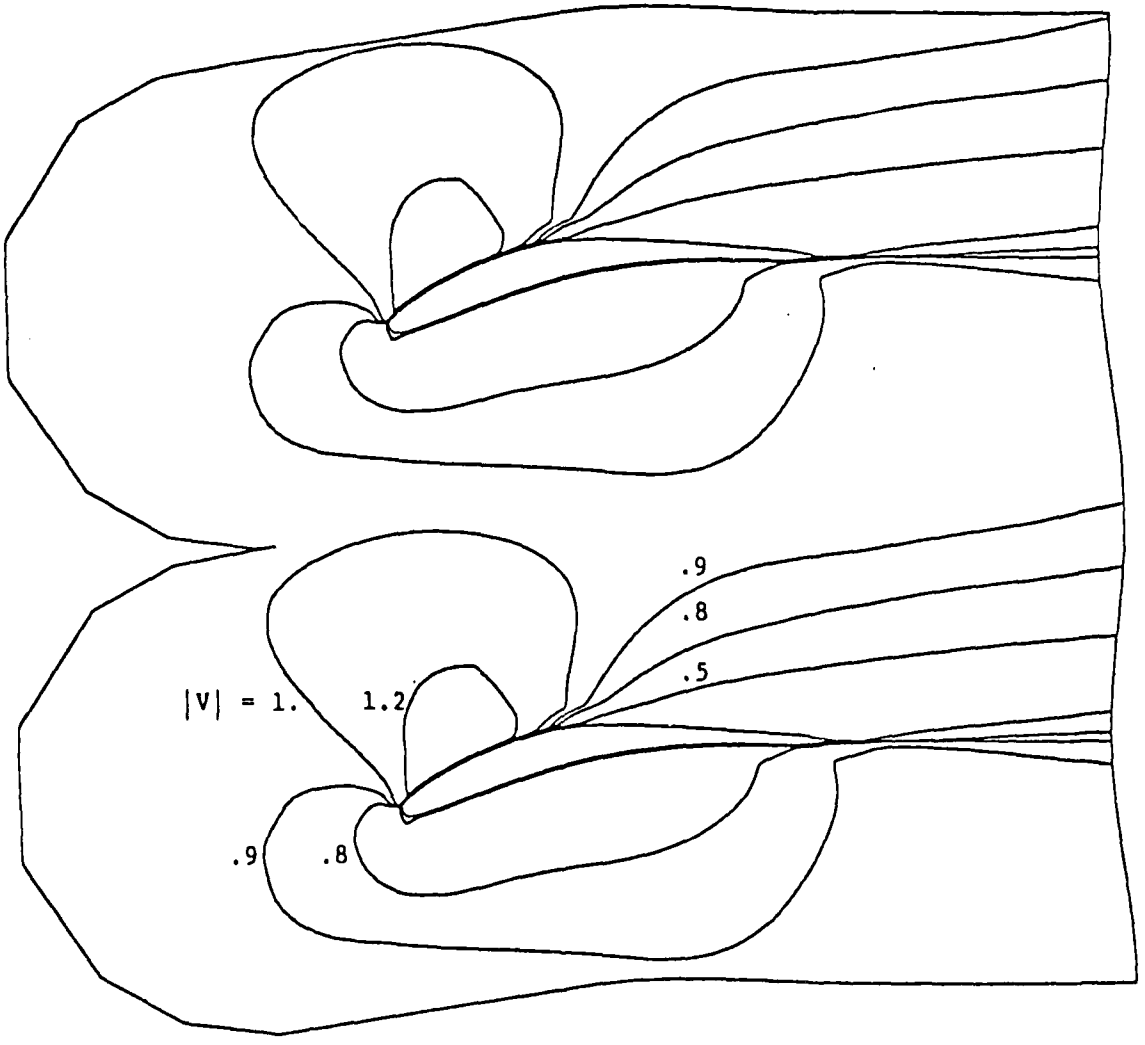

Fig. 15 - Velocity contours, σ = .5.

Fig. 16 - Velocity contours, σ = .05.

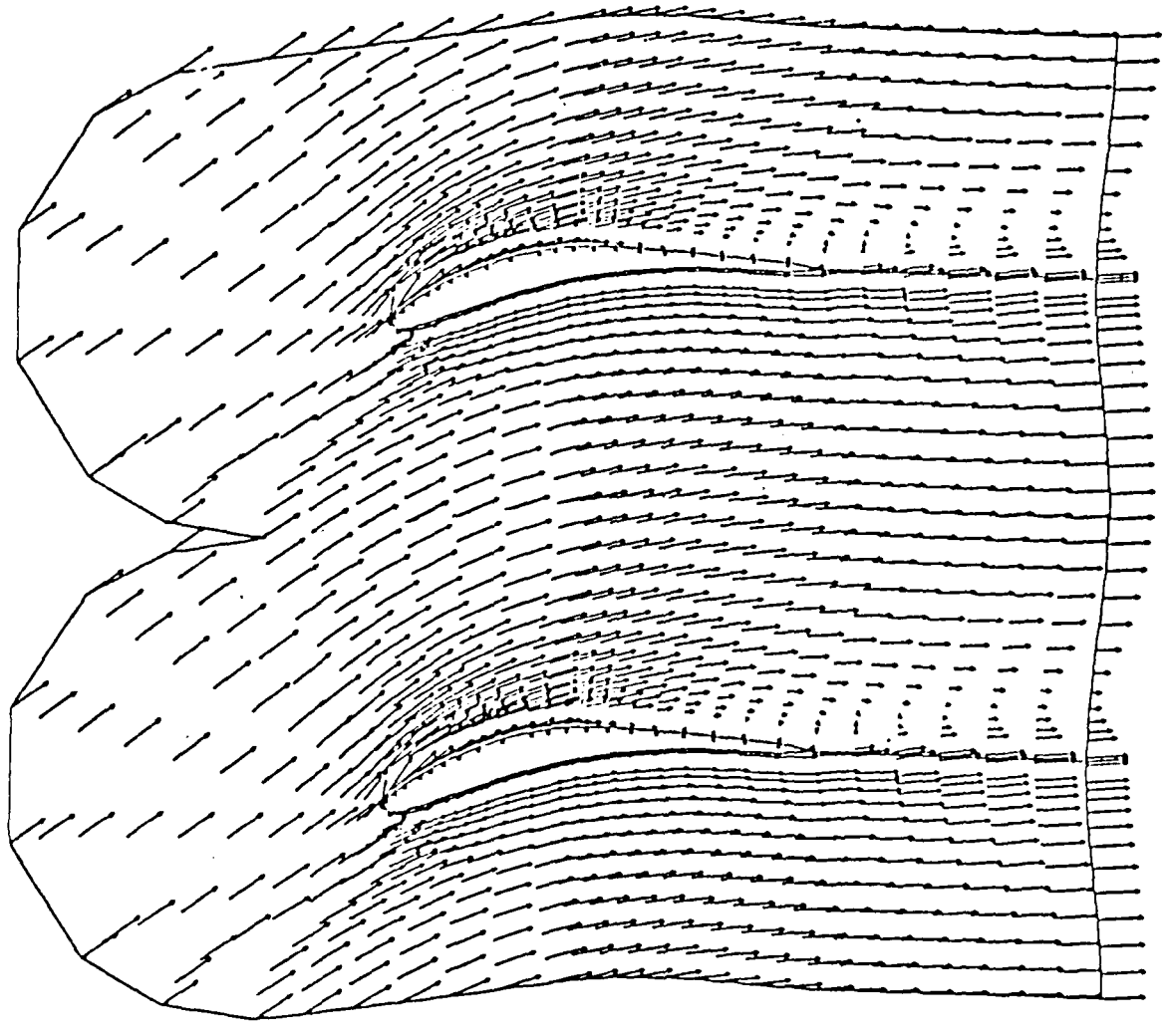

Fig. 17 - Velocity vector plot, $\sigma = .5$.

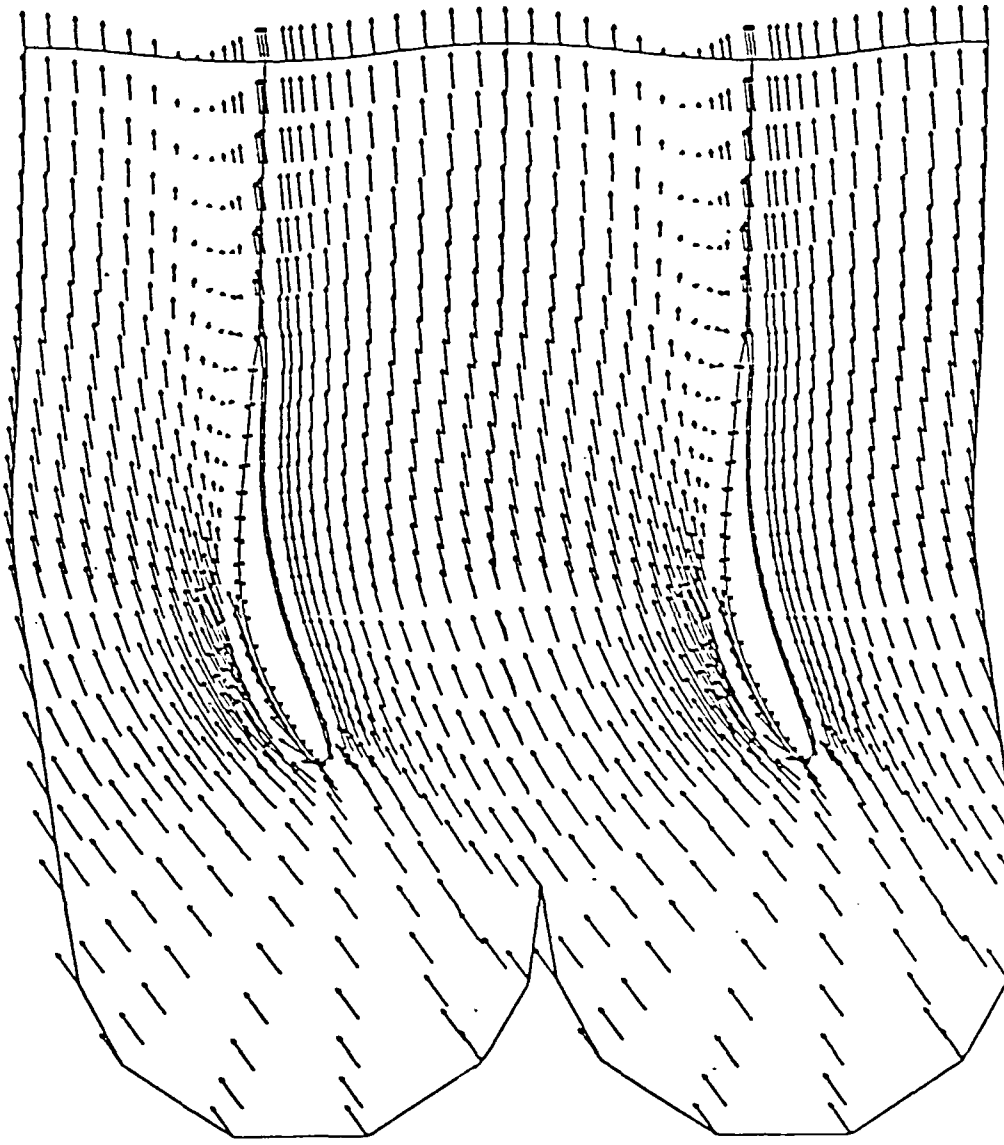

Fig. 18 - Velocity vector plot, σ = .05

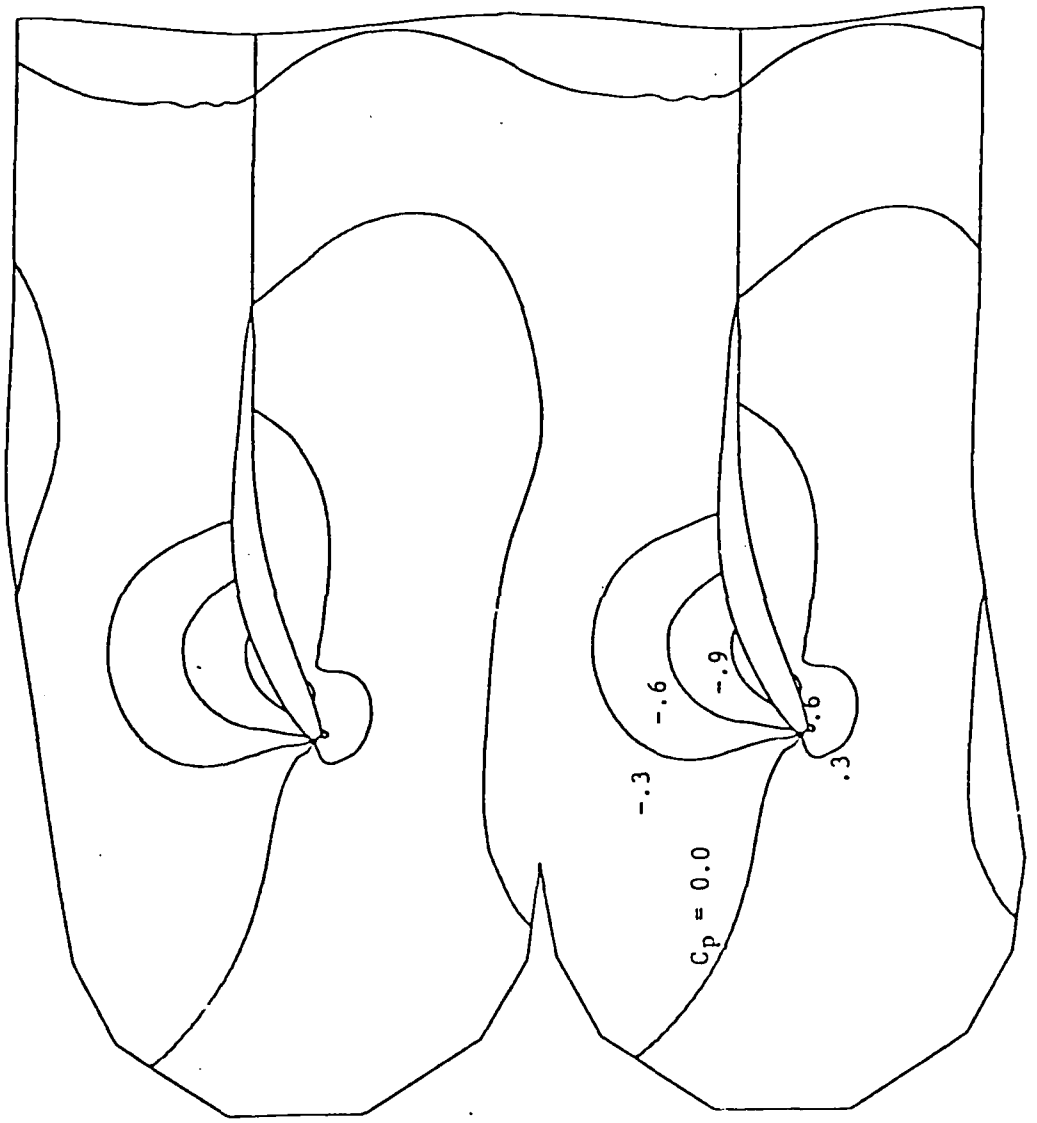

Fig. 19 - Static pressure contours, σ = .5.

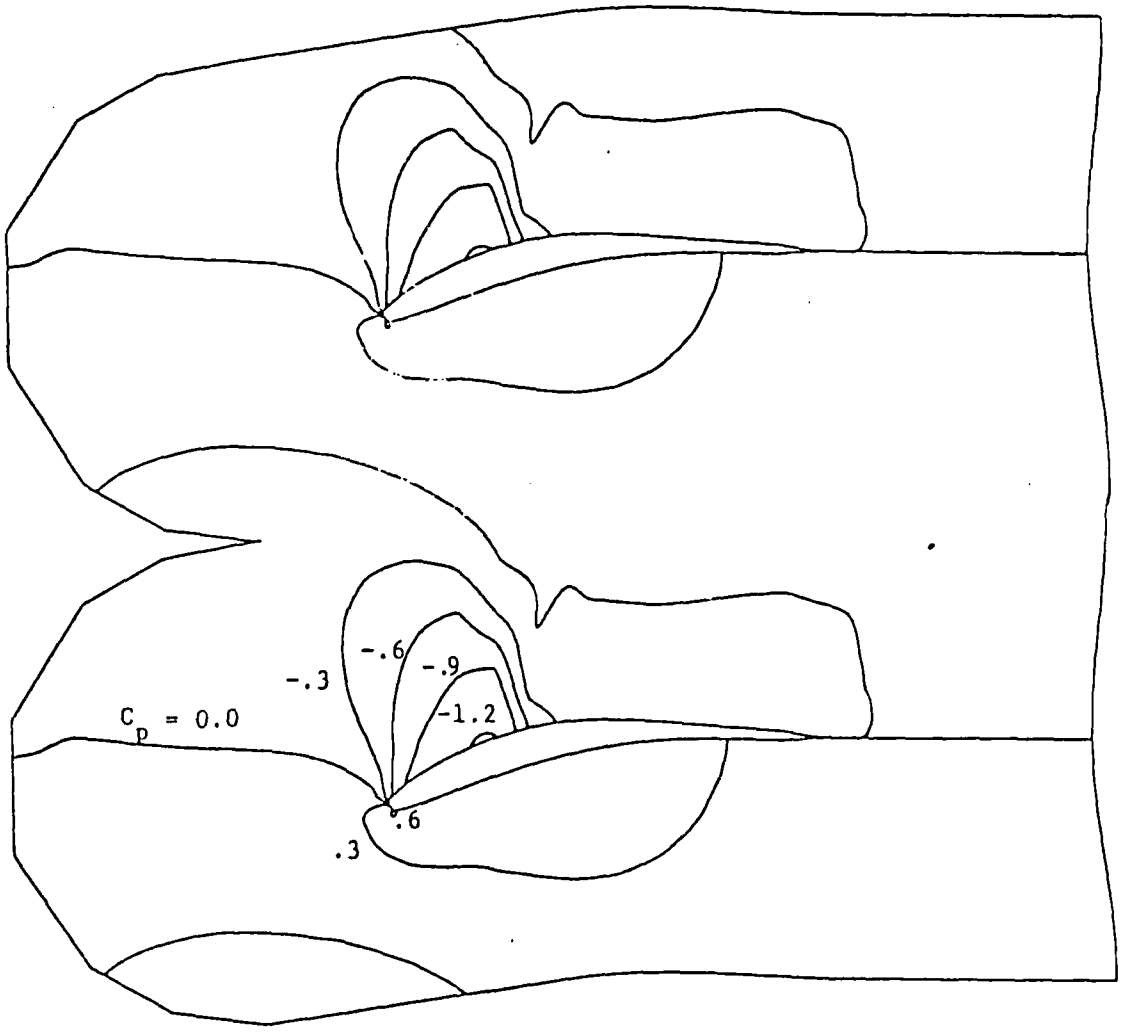

Fig. 20 - Static pressure contours, σ = .05.

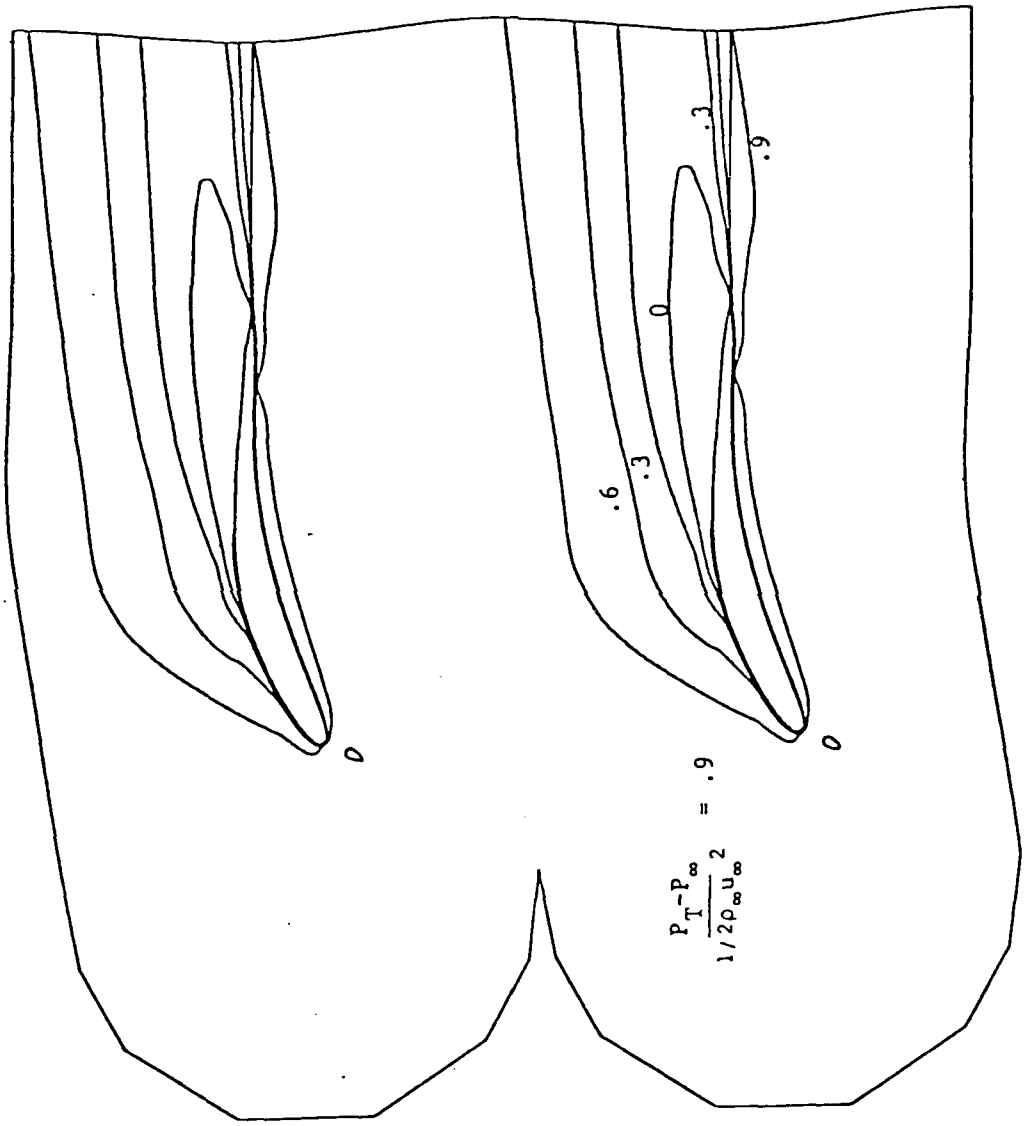

Fig. 21 - Total pressure contours, $\sigma = .5$.

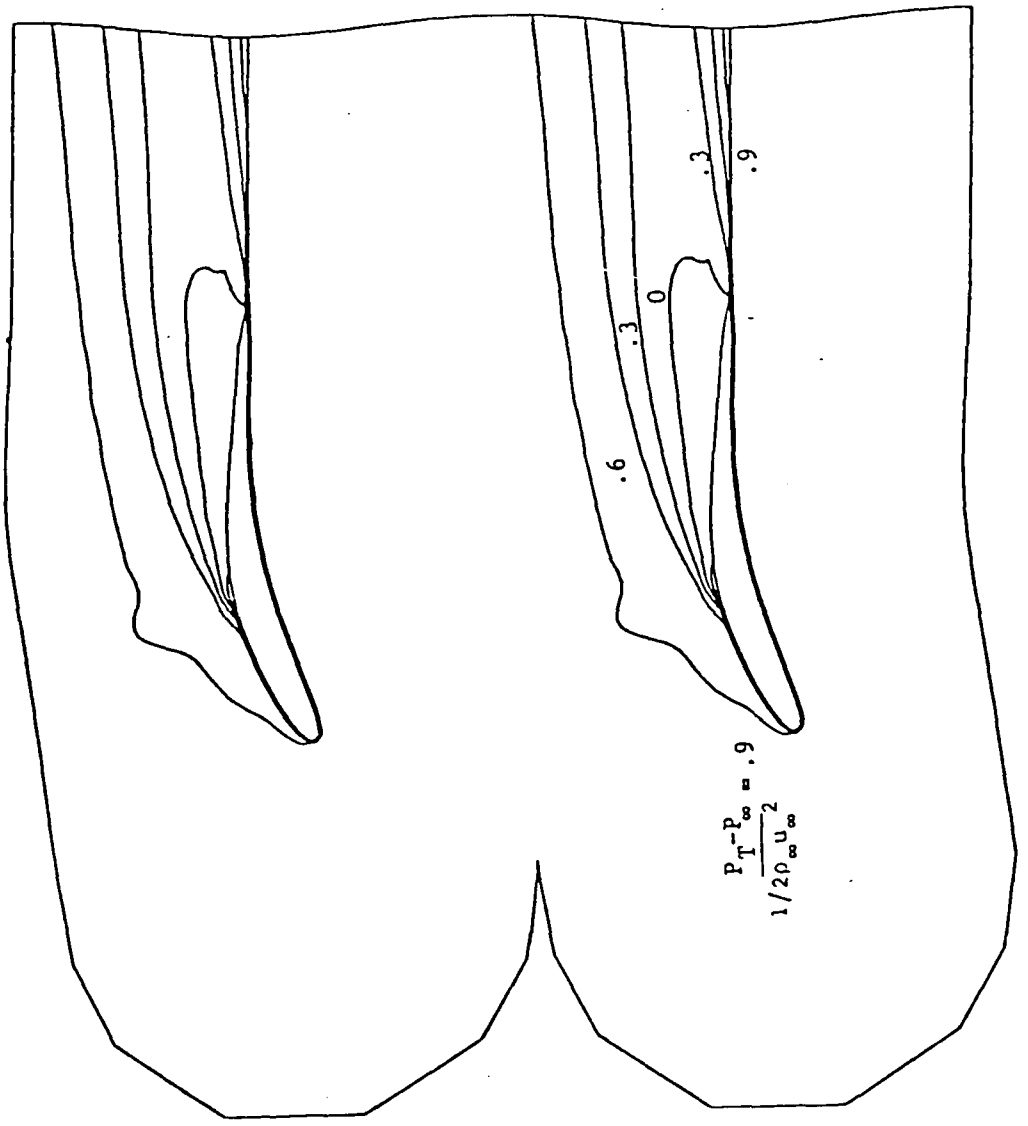

Fig. 22 - Total pressure contours, $\sigma = .05$.


DATE
FILMED
3-8